

Small-angle Neutron Scattering lecture

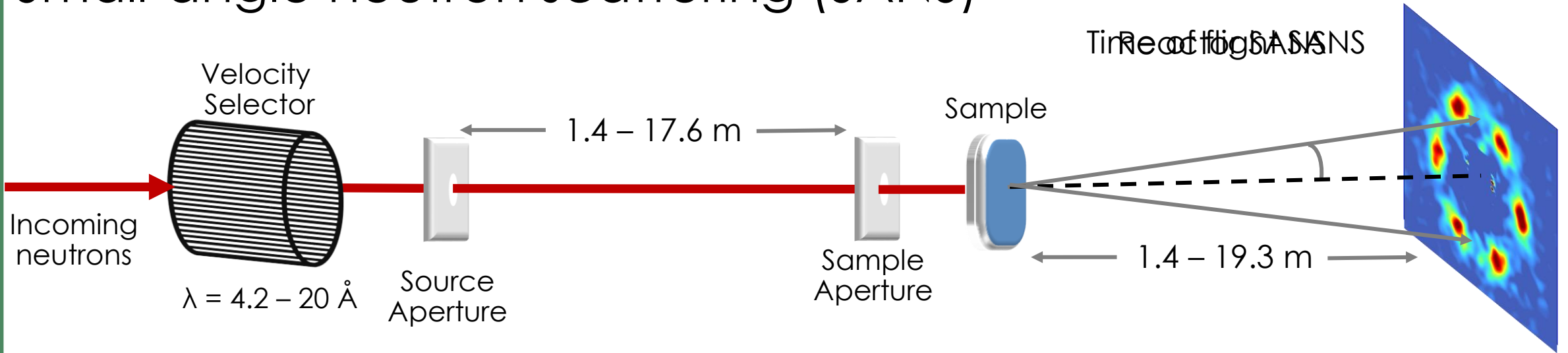
Lisa DeBeer-Schmitt
NXSchool July 2022

ORNL is managed by UT-Battelle, LLC for the US Department of Energy

Outline:

- What is SANS?
- Instruments at ORNL
- Sample Environment capabilities
- Science Cases
 - Polymers
 - Magnetic ordering (diffraction)
 - Engineering materials
- New Directions

Small-angle neutron scattering (SANS)



Scattering length density

$$I(Q) = A \Delta\rho^2 n V^2 P(Q) S(Q)$$

Calibration

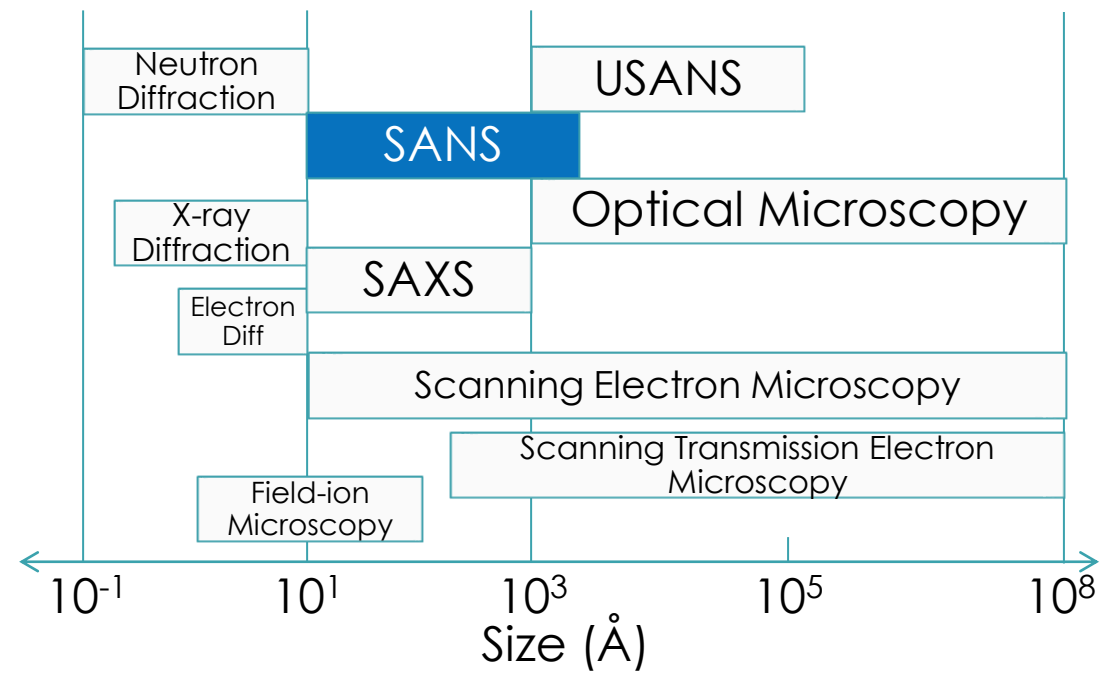
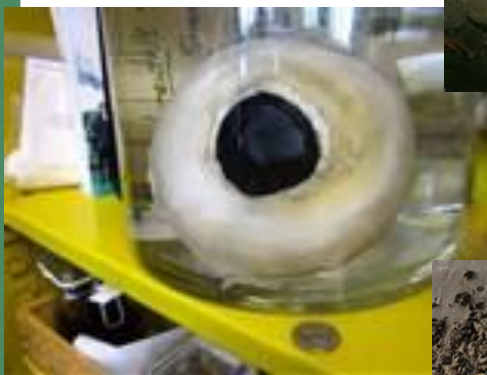
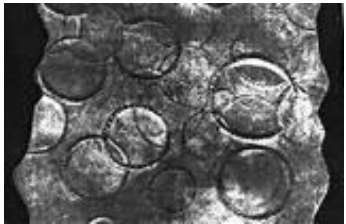
Form and structure factors

Probes lengths of 0.5 - 700 nm
 Using angles of $\theta = <0.1$ to 45°

A powerful tool for studying nanophase bulk materials

SANS with other techniques

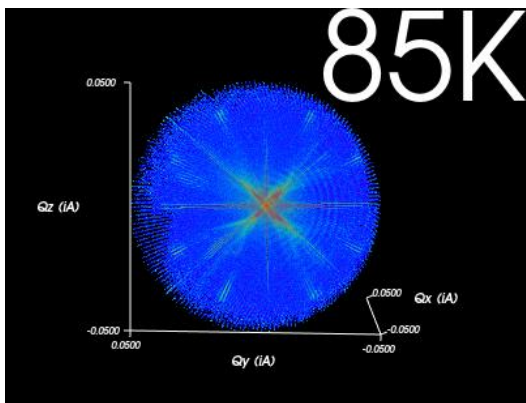
Microscopy: Direct but limited



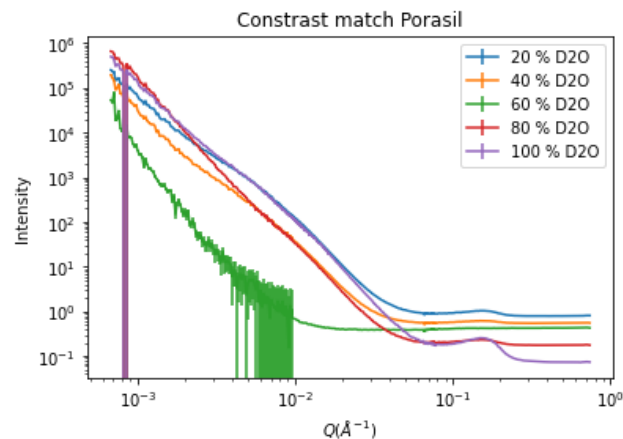
SAS: Indirect and model-dependent but in-situ

Why Neutrons?

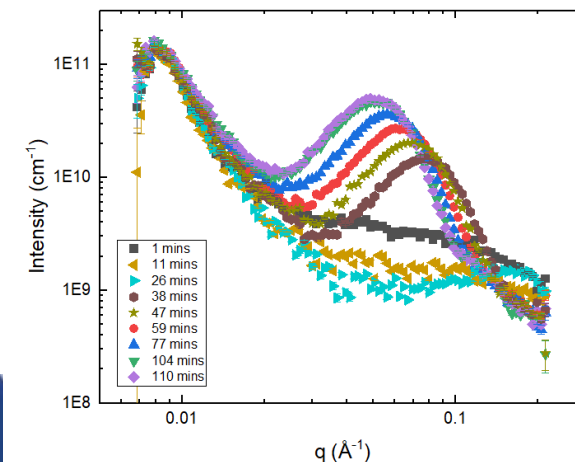
- Low Energy ($E=80\text{meV}$ for 1 \AA neutrons vs. 12.42 keV for x-rays. **No radiation damage.**)
- High Penetration of cold neutrons – bulk samples
- Large difference in the scattering cross-section for the hydrogen and deuterium- contrast variation capability.
 - Solute or solvent can be deuterated to vary the contrast ($\rho_{\text{H}_2\text{O}} = -0.56 \times 10^{10} \text{cm}^{-2}$, $\rho_{\text{D}_2\text{O}} = 6.334 \times 10^{10} \text{cm}^{-2}$)
 - Study of multicomponent systems through selective deuteration and contrast matching with H/D mixtures.
- Sensitive to substantial difference in scattering length density in transition metals
- **MAGNETISM.**
 - Neutron has a magnetic moment and spin which give contrast



Magnetic domains in FeV_2O_4
L. Kish et al in preparation



Data from NXschool experiment

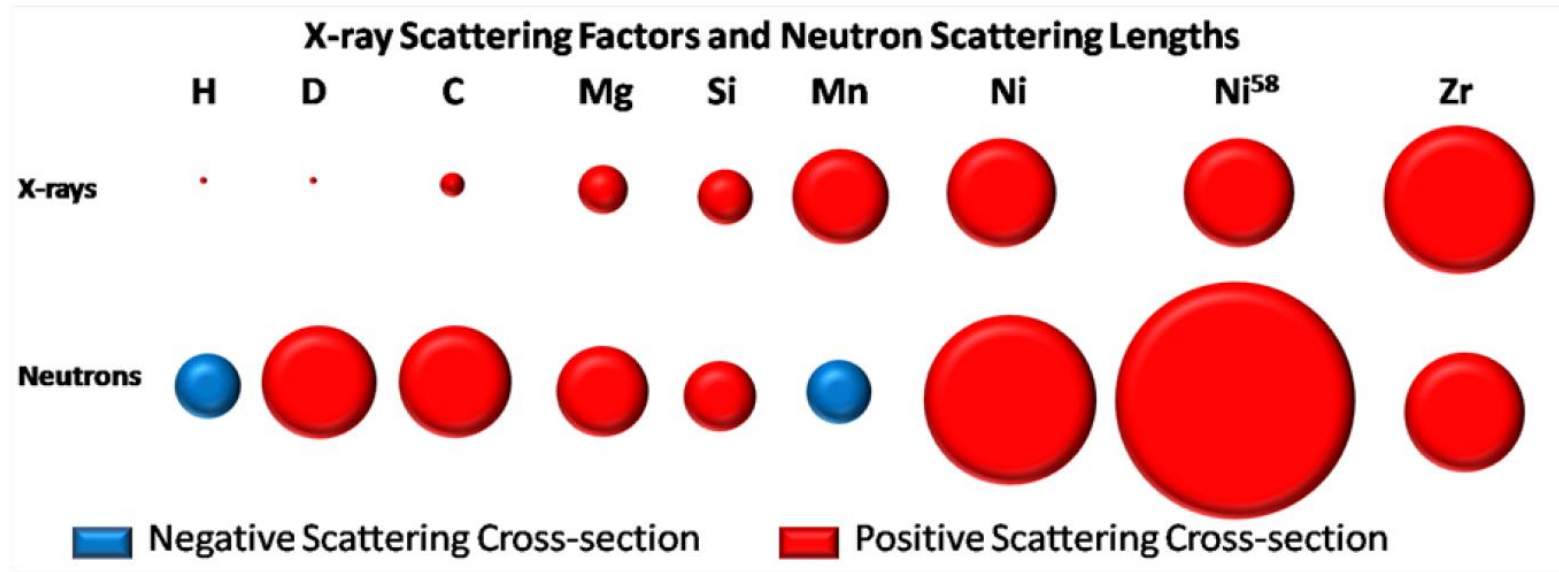


Copper precipitate growth in steel

Neutron and x-ray scattering cross-sections

X-ray and neutron scattering are essentially the same concept, except...

- X-rays scatter from electrons
- Neutrons scatter from nuclei

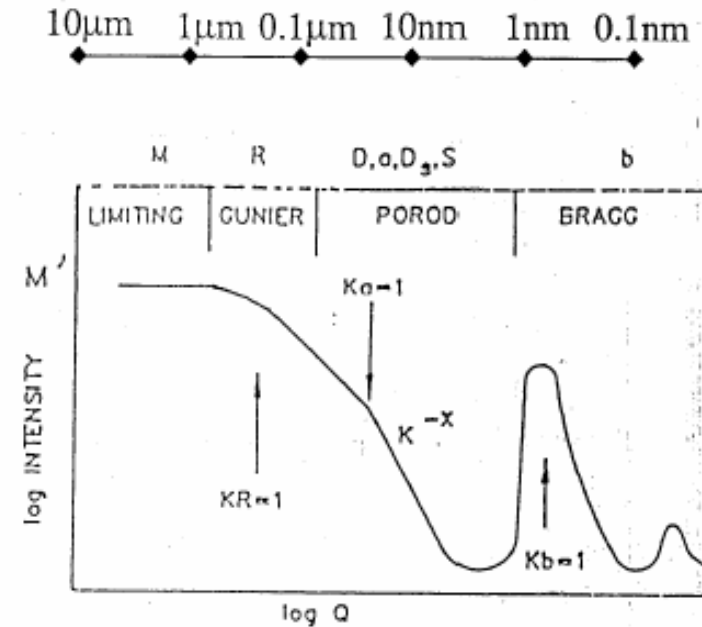
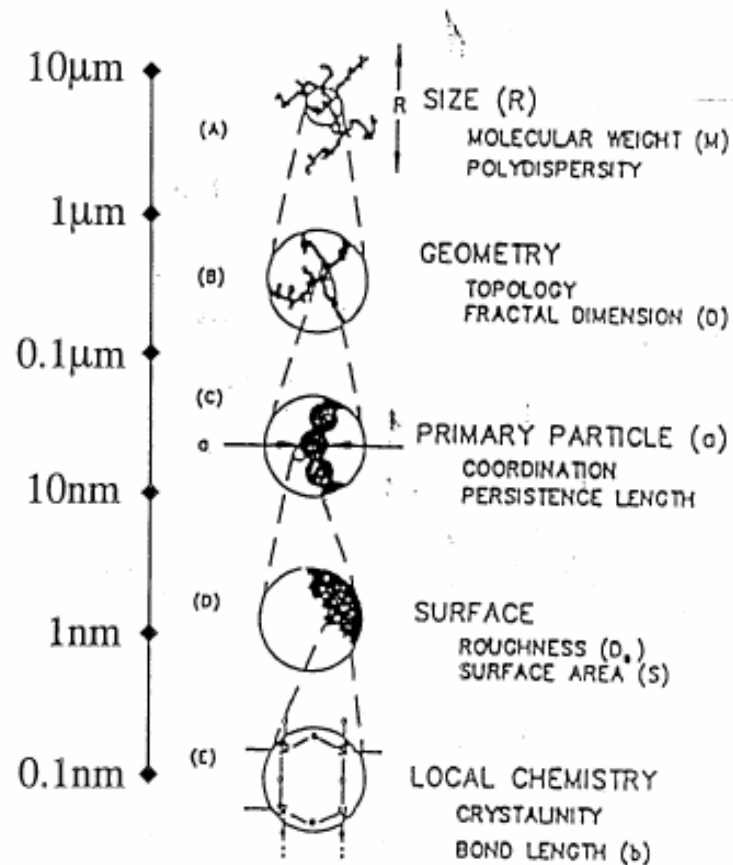


<http://www.ncnr.nist.gov/resources/n-lengths/>

http://www.isis.rl.ac.uk/ISISPublic/reference/Xray_scalfac.htm

C. Metting, Dissertation University of Maryland 2011

SANS from hierarchical structures



SANS is a structural technique that probes a wide array of length scales

SANS Suite



ORNL SANS instrument specifications.

	GP-SANS	Bio-SANS	EQ-SANS	USANS
Moderator	Supercritical hydrogen	Supercritical hydrogen	Coupled, supercritical hydrogen	Decoupled, poisoned hydrogen
Source	Reactor, continuous	Reactor, continuous	Spallation, 60 or 30 Hz, TOF	Spallation, 60 Hz, TOF
Sample-to-detector distance	1.1–20 m	1.1–15.5 m	1.0–9 m	N/A
Beam size	Up to 20 mm diameter	Up to 20 mm diameter	Up to 15 mm diameter	Up to 40 mm by 40 mm
Q range	7×10^{-4} to 1 \AA^{-1}	9×10^{-4} to 1 \AA^{-1}	2×10^{-3} to 6 \AA^{-1}	7×10^{-6} to $5 \times 10^{-3} \text{ \AA}^{-1}$
Incident wavelength	4–25 \AA	6–25 \AA	0.5–20 \AA	3.6, 1.8, 1.2 and 0.9 \AA
$\Delta\lambda/\lambda$	9–45%	9–45%	<1–20% †	Monochromated with crystals
Detector type	^3He LPSD array	^3He LPSD array	^3He LPSD array	^3He

† The resolution of EQ-SANS is wavelength dependent and also depends on the binning used in the software. The upper end of the range indicated is for the shortest wavelength used in the current data reduction.

Sample Environments:

Current Sample environment options:

- A suite of changers that can be configured to hold from 8 -18 samples
- Peltier system that goes from -10 to 120 °C with 0.01 degree control and holds 12 samples.
- HiDRA load frame; rheometer
- Shared furnace capable of temperature up to 200 °C
- New controlled atmosphere furnace and vacuum furnace to > 1000 °C
- Horizontal 11 T recondensing magnet allowing users to utilize 11 T at 30 mK. (3/2016), 5 T horizontal open bore magnet (5/2017) and 8 T vertical magnet with temps 30 mK to 300 K
 - Electric field and current can also be applied to the samples
- SANS dedicated cryostat with sapphire windows
- Pressure cells (McHugh 2kBar and 1kBar changer)

Future upgrades:

- Strain cell to apply in-situ compression or tension (11 T and 5 T magnets)
- In-situ reaction vessel
- Load frame for stretching polymers



Science cases

- Diblock copolymers
- Skyrmion in thin films
- Novel Steels for reactor



Influence of Cleavage of Photosensitive Group on Micellization and Gelation of a Doubly Responsive Diblock Copolymer

Lilin He¹, Bin Hu², Daniel M. Henn², and Bin Zhao²

¹ Large Scale Structure Group, Neutron Scattering Division, Oak Ridge National Laboratory

² Department of Chemistry, University of Tennessee: Knoxville

ORNL is managed by UT-Battelle, LLC for the US Department of Energy



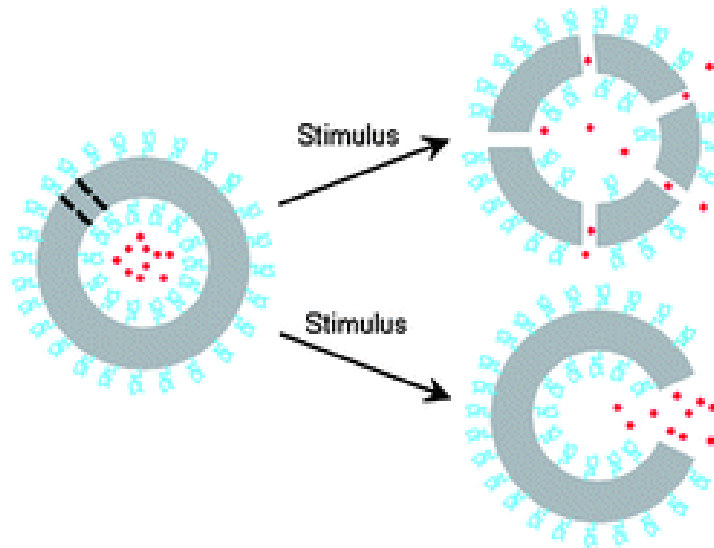
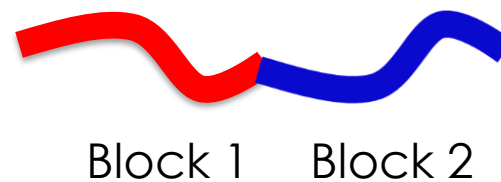
THE UNIVERSITY OF
TENNESSEE
KNOXVILLE



U.S. DEPARTMENT OF
ENERGY

Influence of Cleavage of Photosensitive Group on Micellization and Gelation of a Doubly Responsive Diblock Copolymer

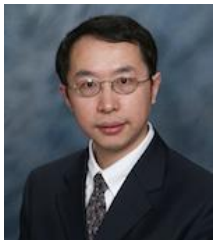
Block Copolymers have wide technical applications owing to their capabilities to self-assemble into nanostructures under different conditions.



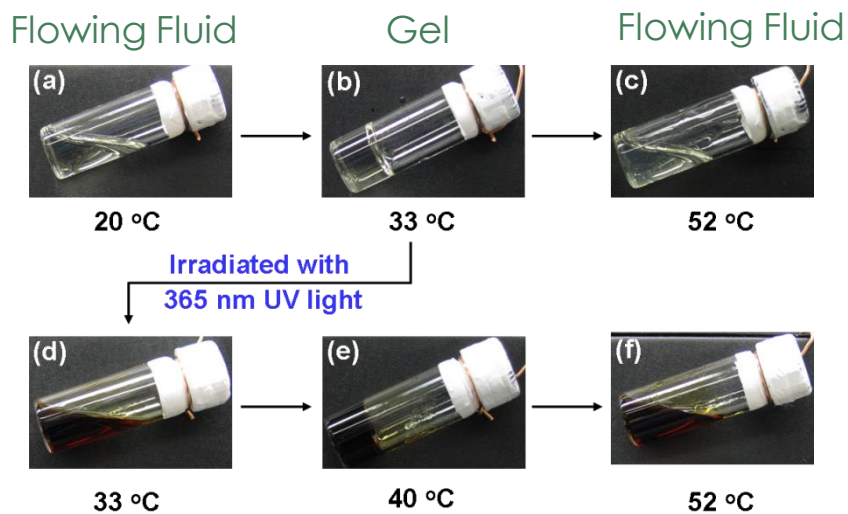
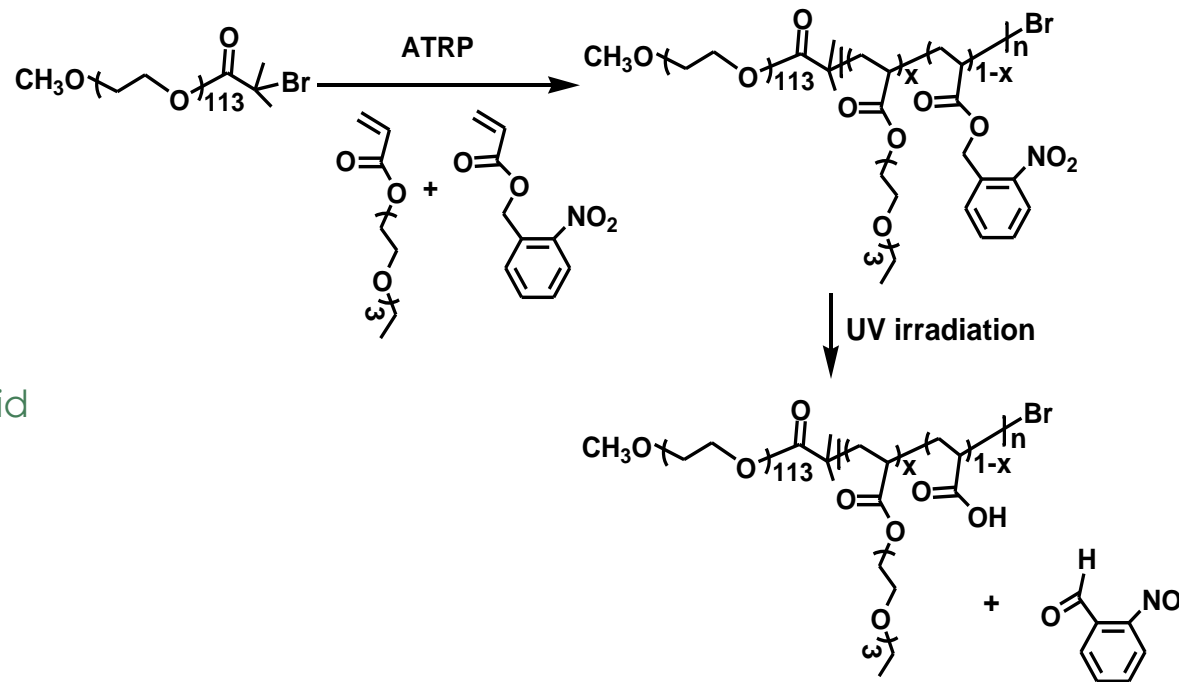
Controlled release example

Challenge: To precisely **tune** and **control** the molecular characteristics of the block copolymers under appropriate conditions.

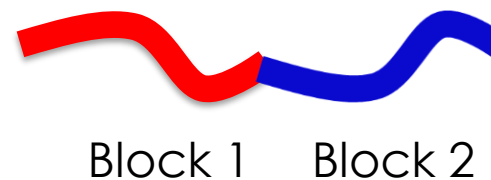
Thermal- and light-sensitive diblock copolymer PEO-b-P(TEGEA-co-NBA)



Prof. Bin Zhao, UTK

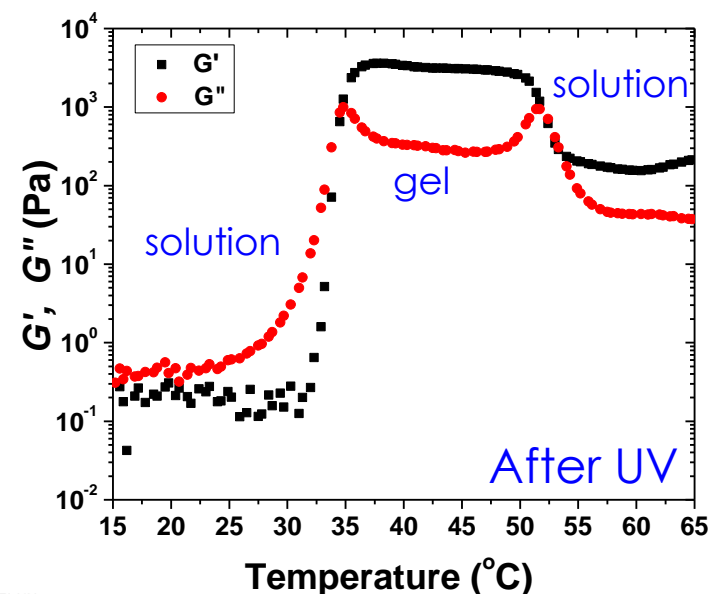
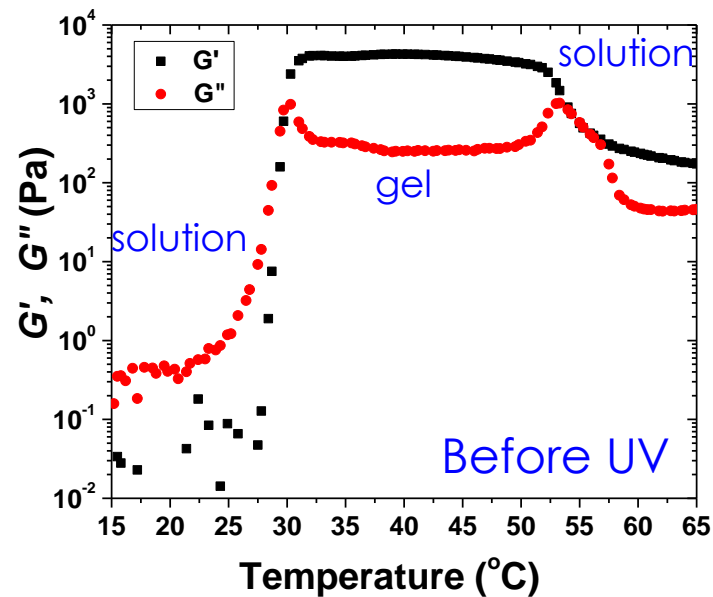


- “living”/controlled radical polymerization
- Irradiated for 6 days with 365nm UV light



- Brown-red color due to the photochemical reaction
- Multiple transitions

Rheological Results



- Dynamic storage modulus G' , loss modulus G'' , versus temperature
- 25wt % D_2O solution of PEO-*b*-P(TEGGA-co-NBA).
- A heating rate of $3^\circ\text{C}/\text{min}$.
- A strain amplitude of 1 %
- An oscillation frequency of 1 Hz.

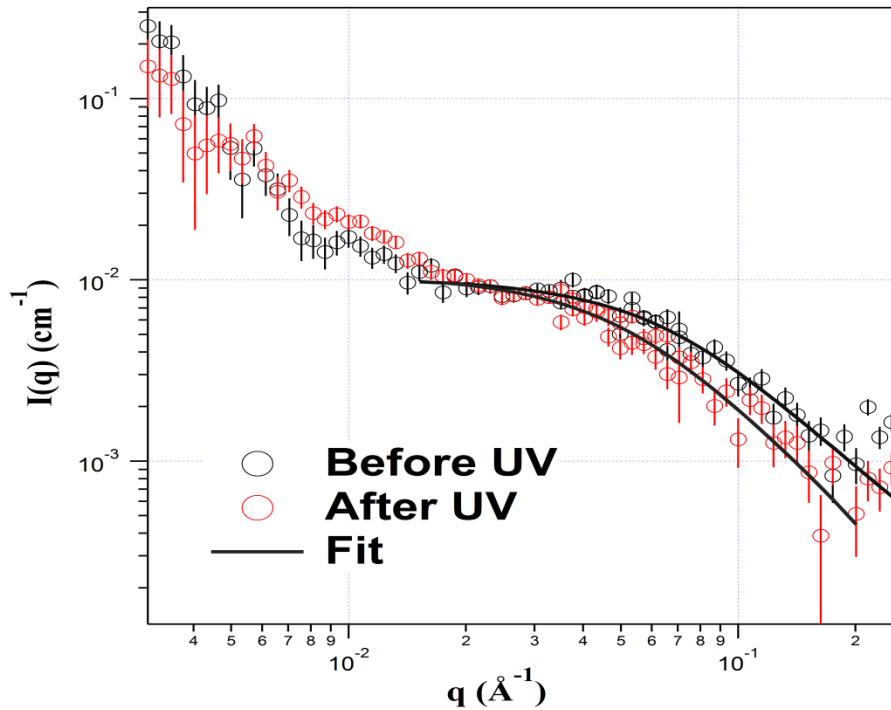
- Reversible sol-gel-soft gel transitions is achieved;
- Gel is composed of packed micelles;
- UV irradiation leads to a narrower gel state window.

Rheological
Properties



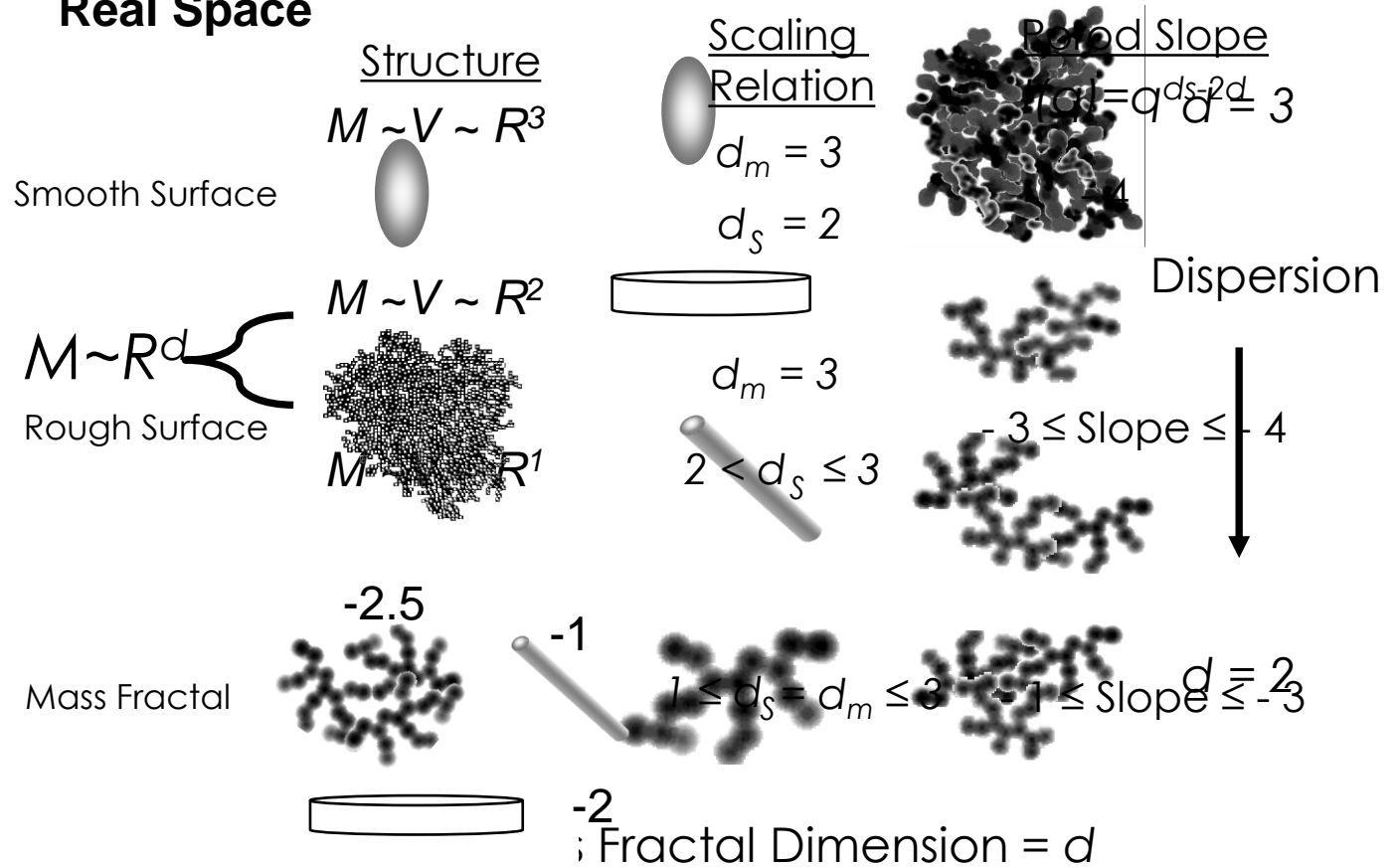
Microstructure

SANS results: Unimer State



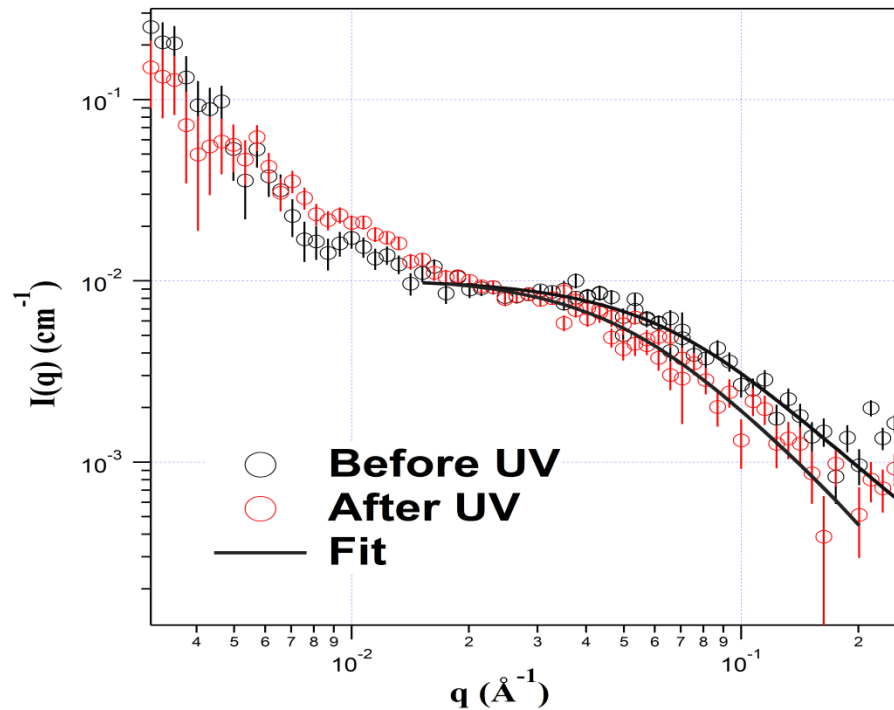
- Guinier Approximation at low-q:
 - $I(Q) = I(0) \exp(-Q^2 R_g^2/3)$
 - $\ln[I(Q)]$.vs. Q^2 plot where $Q.R_g < 1.0$
 - $R_g = \sqrt{(3 \cdot \text{slope})}$
 - $M = (1000 \cdot I(0) \cdot d^2 \cdot N_A) / (C \cdot \Delta\rho^2)$
- Power-law at high q

Real Space



Lilin He, et al. **Polymer**, Volume 105, 25-34 (November 2016) <https://doi.org/10.1016/j.polymer.2016.10.019>

SANS results: Unimer State



- 0.02wt%
- 15 °C

A model for polymers with excluded volume fraction yields R_g and Porod exponent

Before UV

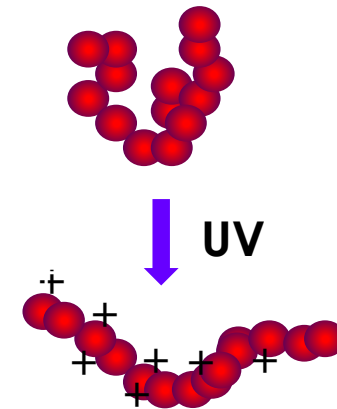
$$R_g = 25.5 \text{\AA}$$

$$\text{Porod exponent} = 1.94$$

After UV

$$R_g = 31.1 \text{\AA}$$

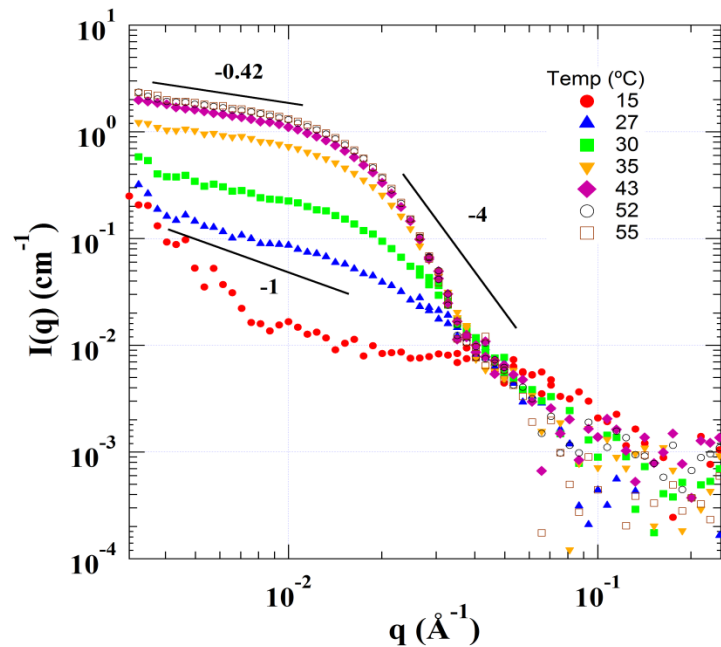
$$\text{Porod exponent} = 1.59$$



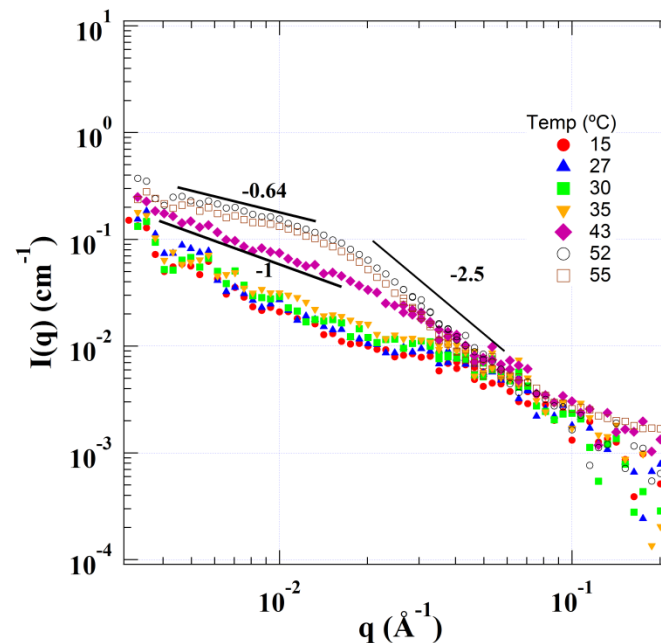
- Both solutions contain single chains and loosely-assembled clusters
- The chains are more stretched after UV irradiation

Temperature Effect: dilute solution

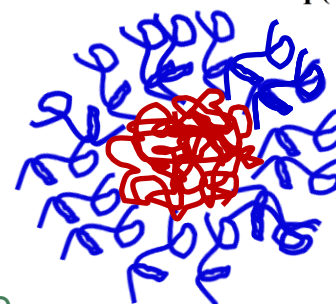
Before UV



After UV

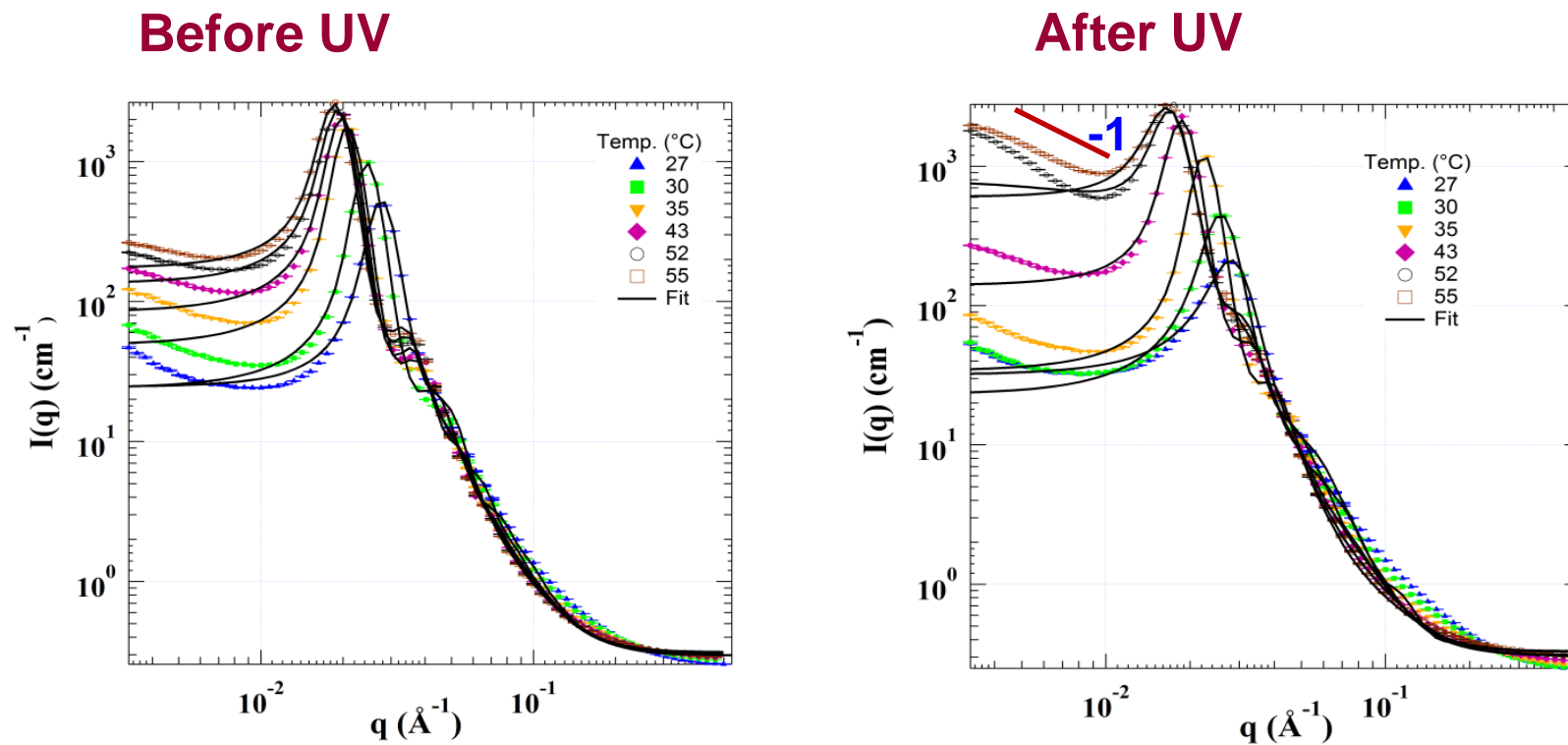


0.02wt%



- Micelles form above critical micelle temperature
- Cleaving the light sensitive group defers the formation of the micelles

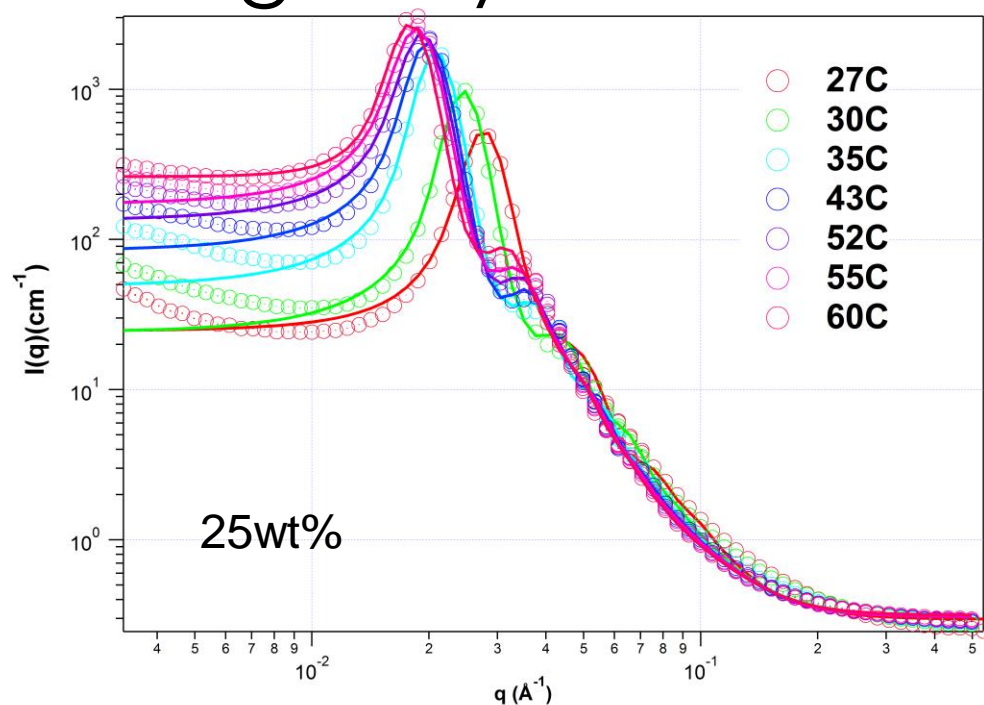
Temperature Effect: Concentrated solution



25 wt%

- Micelles grows with temperature;
- Possible sphere to rod transition at 55C for the UV exposed sample.

Model Fitting: Polycorshell model



$$\frac{d\Sigma(Q)}{d\Omega} = \Delta\rho^2 \phi V_p P(Q) S(Q)$$

Percus-Yevick closure of the Ornstein-Zernike equation

Material Balance Calculation

$$N_{ag}(131 \cdot v_{TN} + 113 \cdot v_{PEO} \cdot f) + 30 \cdot c = \frac{4\pi}{3} R_A^3$$

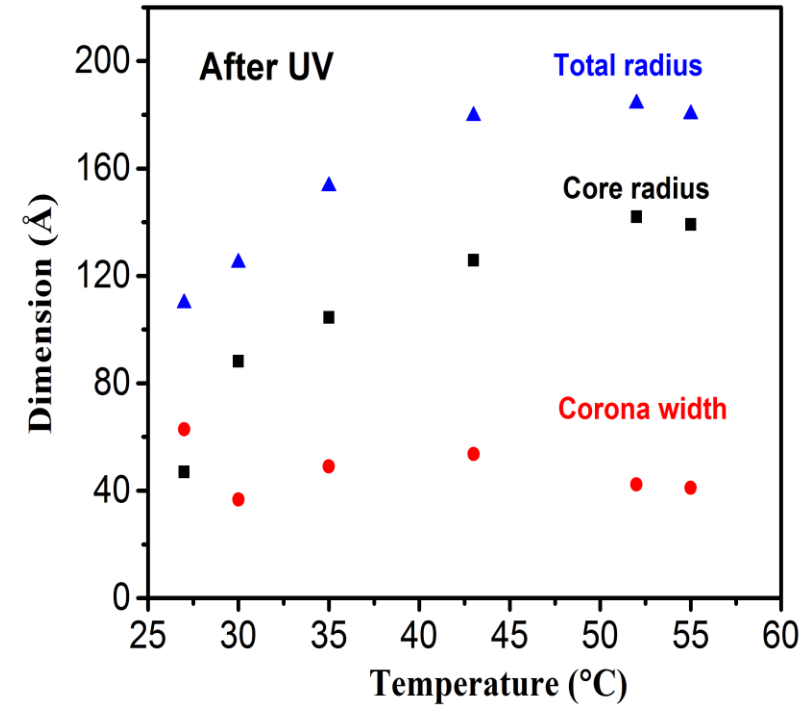
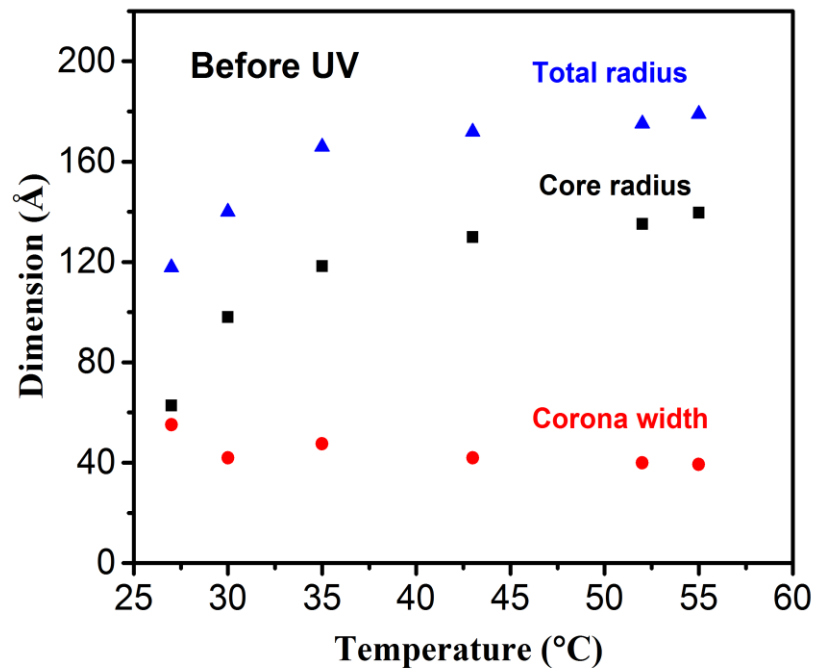
$$N_{ag} \cdot 113 \cdot v_{PEO} \cdot (1-f) + 30 \cdot d = \frac{4\pi}{3} (R_B^3 - R_A^3)$$

$$N_{ag}(131 \cdot b_{TN} + 113 \cdot b_{PEO} \cdot f) + 191 \cdot c = \frac{4\pi}{3} R_A^3 \cdot \rho_A$$

$$N_{ag} \cdot 113 \cdot b_{PEO} \cdot (1-f) + 191 \cdot d = \frac{4\pi}{3} (R_B^3 - R_A^3) \cdot \rho_B$$

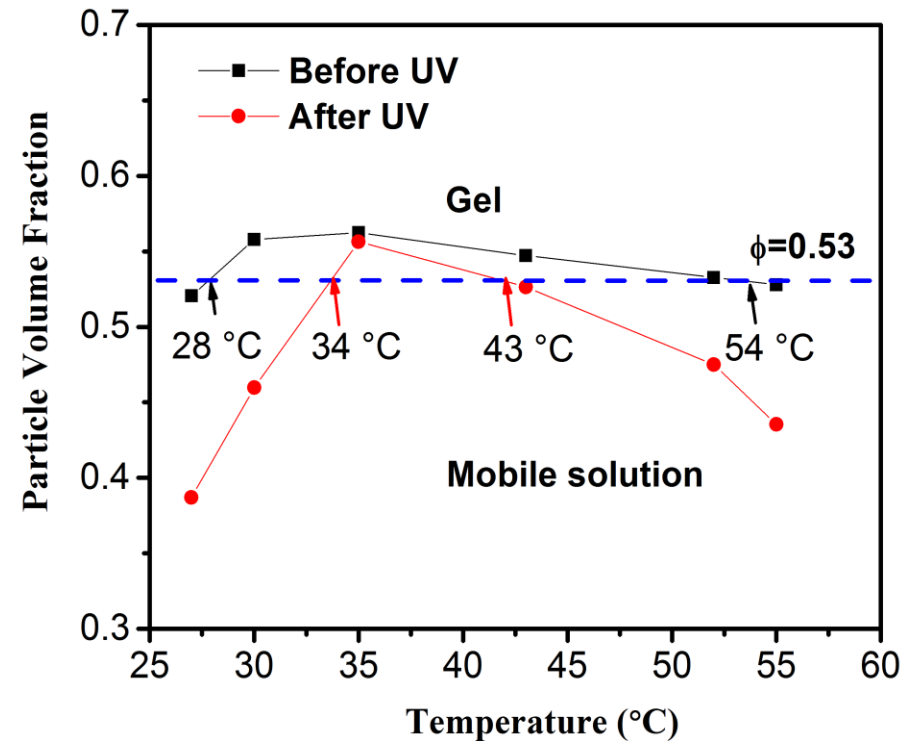
- **Micelle size (core and corona) and volume fraction**
- **Size polydispersity**
- **SLDs in core and corona**
- **Aggregation number**
- **Number of D₂O molecules in core and corona**
- **Fraction of PEO chains in core and corona**

Temperature Effect: Concentration solution



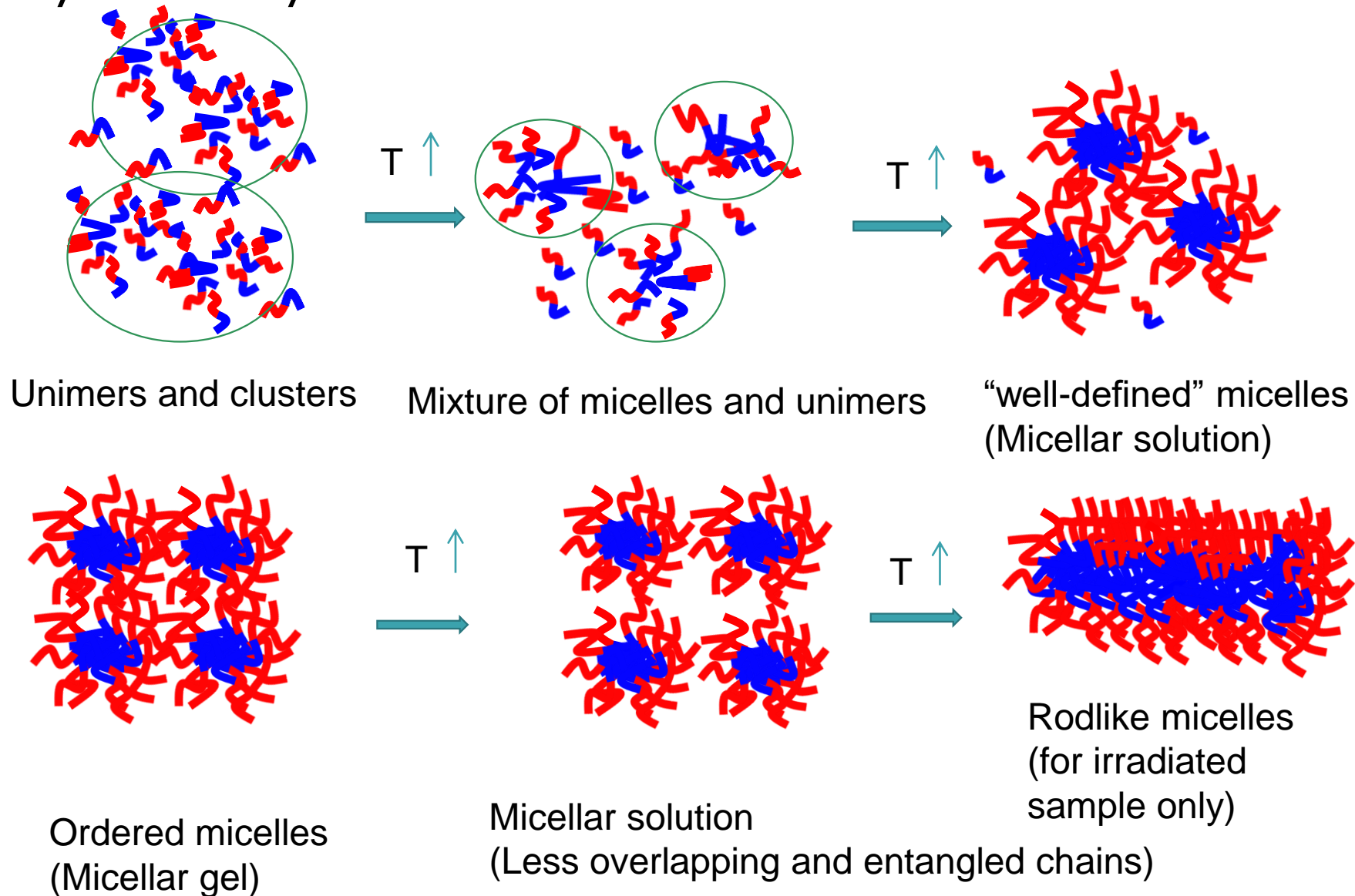
- The core size increases while the corona width remains;
- The slight shrinkage of corona at high temperatures is attributed to the loss of water, which is caused by the reduced miscibility of water and PEO.

Temperature dependence of particle volume fraction



- Micelle effective volume fraction agrees the viscoelastic properties of solutions;
- Delayed gel formation in irradiated sample due to higher LCST transition;
- Critical value 0.53 ± 0.02

Summary of Polymer Micellization



Realization of magnetic skyrmions in thin films at ambient conditions

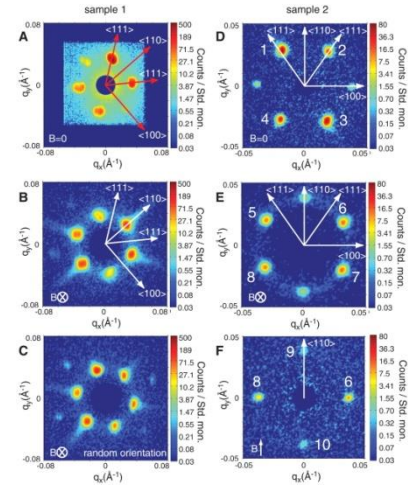
Ryan Desautels, **Lisa DeBeer-Schmitt**, Sergio Montoya, Julie Borchers, Soong-Guen Je, Nan Tang, Mi-Young Im, Micheal Fitzsimmons, Eric Fullerton, Dustin Gilbert

ORNL is managed by UT-Battelle, LLC for the US Department of Energy

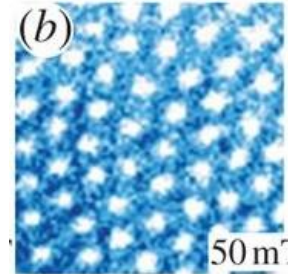
Skyrmions: a brief introduction



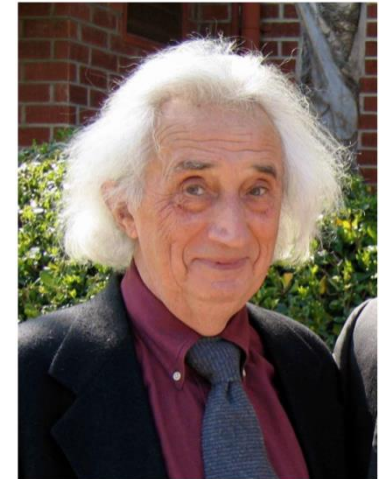
Tony Skyrme
Nuc. Phys. 13, 556 (1962)



Science 323, 915 (2009)

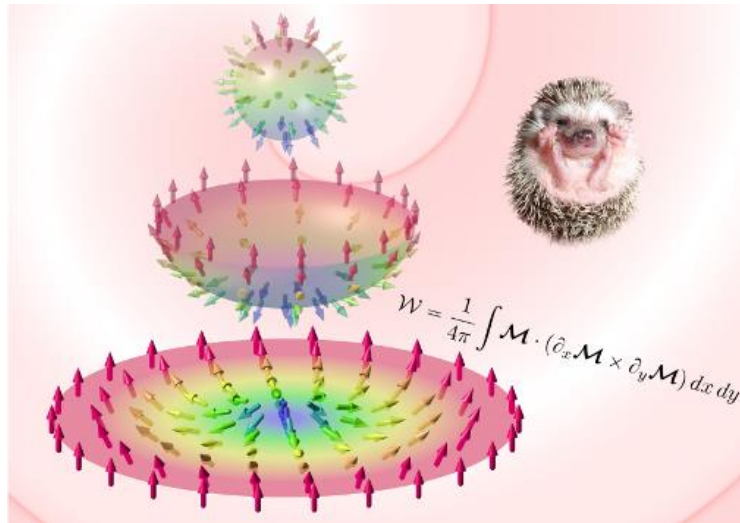


Nature 465, 901 (2010)

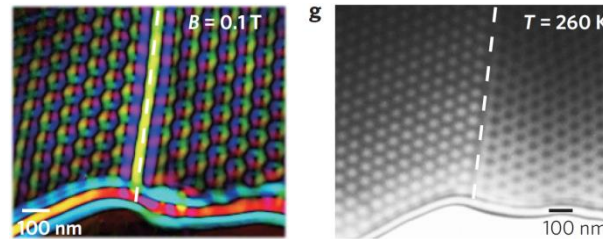


Igor Dzyaloshinskii
Soviet Physocs Jetp. 5, 1259 (1957)

Toru Moriya
Phys. Rev. 120, 91 (1960)



Predicted in magnetic systems
(Phys. Rev. Lett. 87, 037203 (2001))



Nature Mater. 10, 106 (2011)

Direct Exchange Prefers
Parallel Alignment

$$E \propto J(\vec{S}_1 \cdot \vec{S}_2)$$

$E \propto D(\vec{S}_1 \times \vec{S}_2)$
DM Interaction Prefers
90° Orientation
Defines a 'handedness'

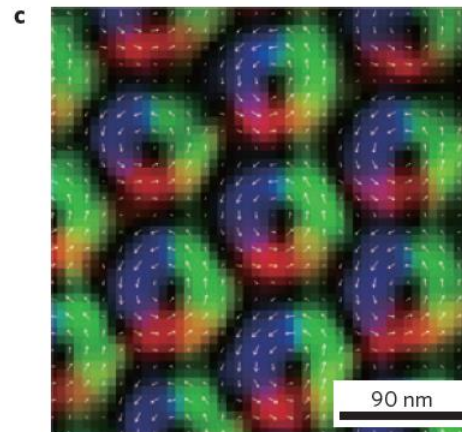
Skyrmions: a brief introduction

Néel (hedgehog)

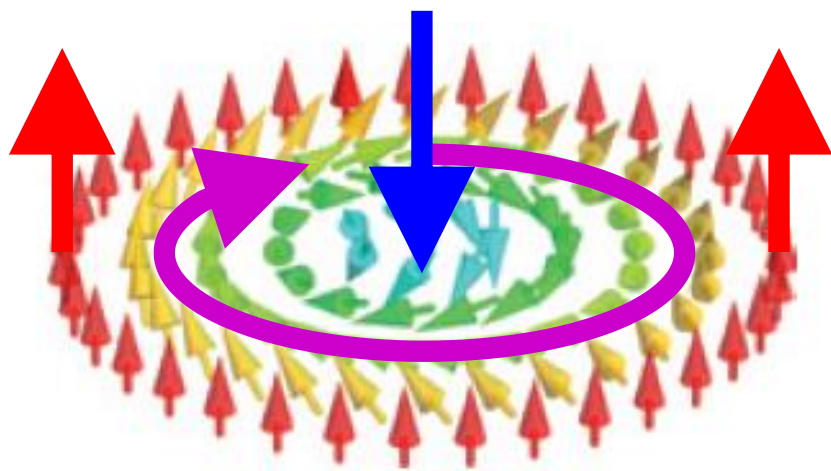


Bloch

(arrows indicate magnetic spins)



Fert, Cros, Sampaio, Nat. Nanotechnol. **8**, 152 (2013).



Circularity (CW and CCW)

Polarity (Core-up, Core-down)
anti-parallel to perimeter

Genus 0



Marble



Bowling Ball

Genus 1



Doughnut



Coffee Cup

Genus 2



Kettle



Scissors

Genus 3 or more



Strainer

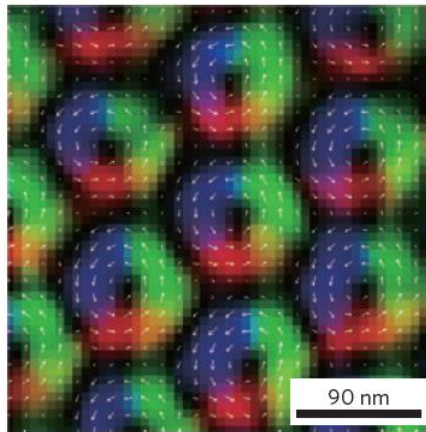
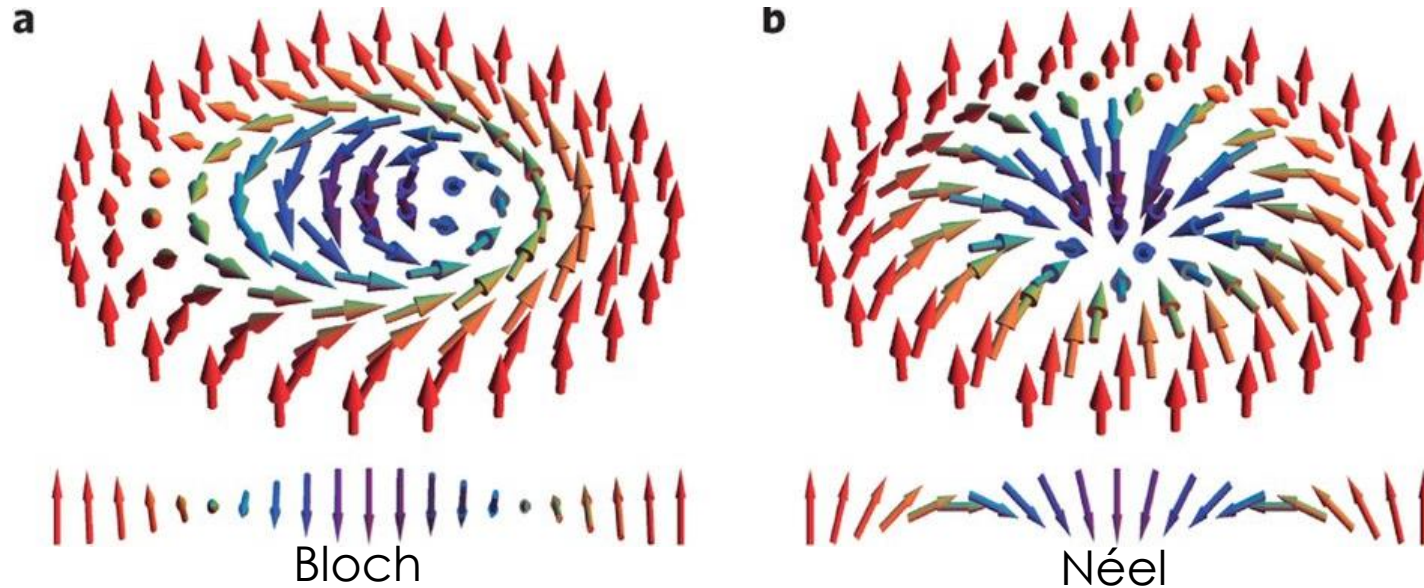


Grater

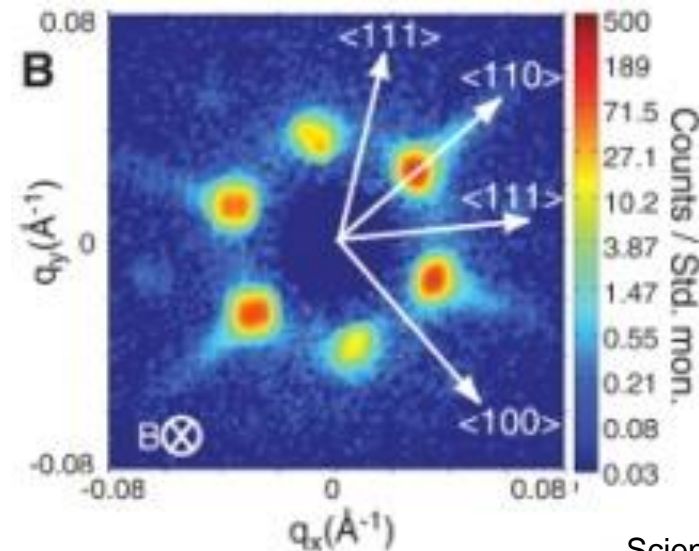
Changing between topological classes
requires irreversible processes

Skyrmions: a brief introduction

I. Kezsmarki et al, *Nature Materials* **volume14**, pages1116–1122 (2015)



Fourier Transform



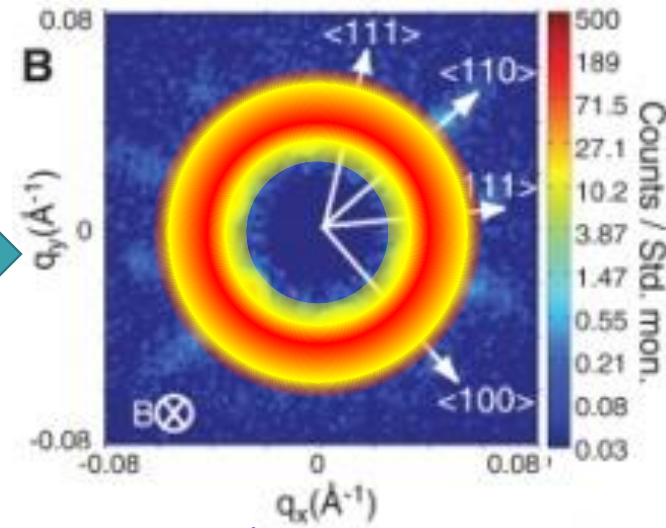
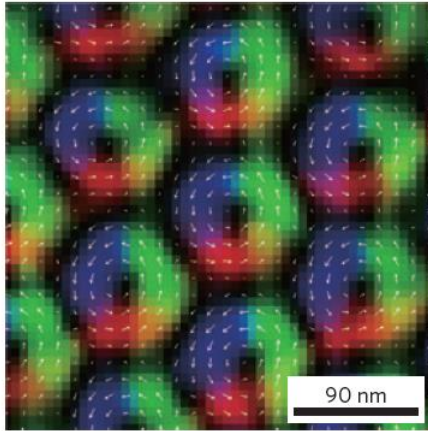
Fert, *Nat. Nanotechnol.* **8**, 152 (2013).

Science 323, 915 (2009)

Magnetism effects on Skymrion stability

Science 323, 915 (2009)

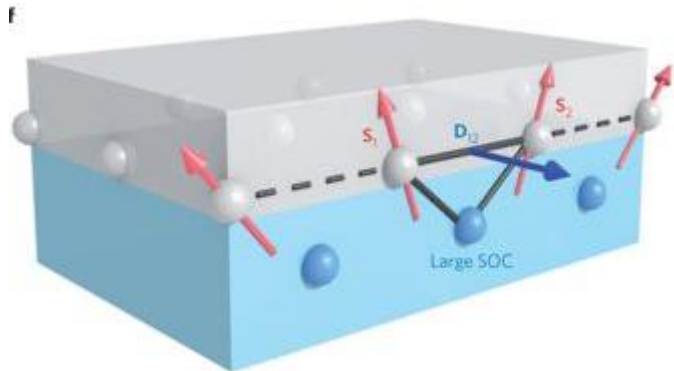
Fert, Nat. Nanotechnol. **8**, 152 (2013).



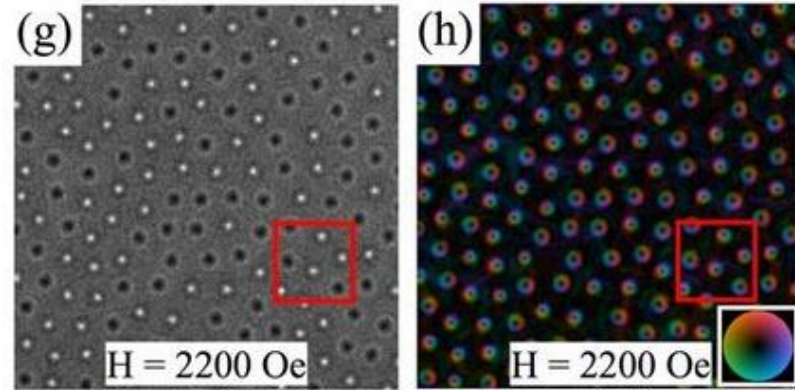
Imagine if we didn't have this long-range ordering...

Origin of the long-range order is in magneto-crystalline coupling

We are interested in skyrmion systems which have weak magnetocrystalline coupling

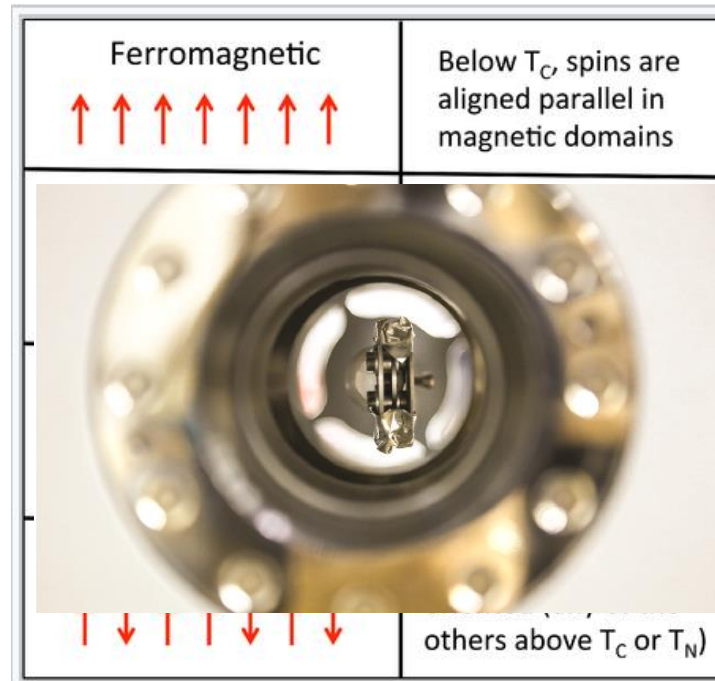
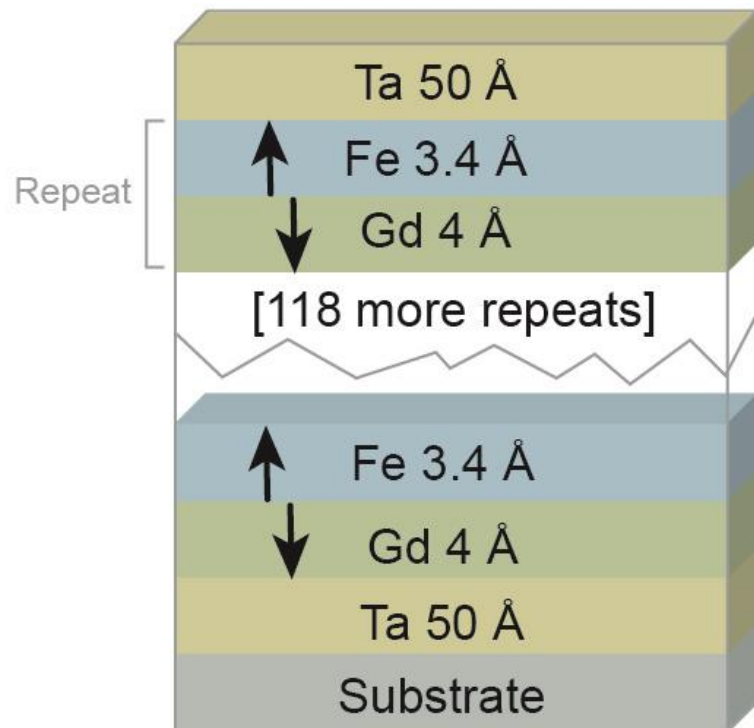


Fert *et al.*, Nat. Nanotechnol. **8**, 152 (2013)



Montoya *et al.*, Phys. Rev. B **95**, 024415 (2017)

Fe/Gd Multilayer Thin Films: The Ingredients for Skyrmions at Ambient Conditions



chem.libretext.org

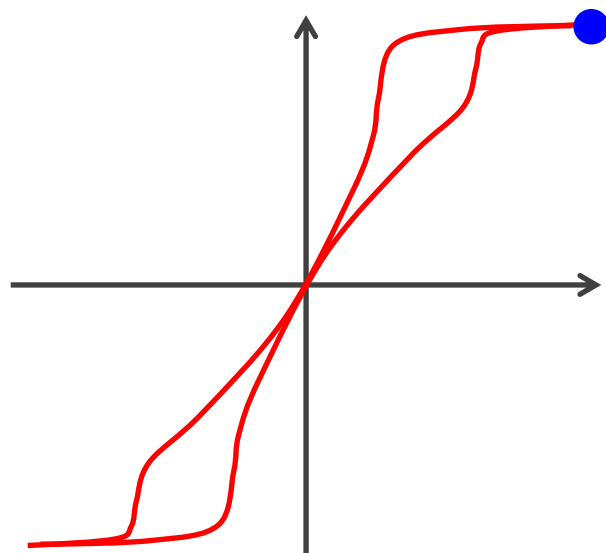
**Ferrimagnetic construction
with perpendicular
magnetic anisotropy**

Dipole-stabilized skyrmions

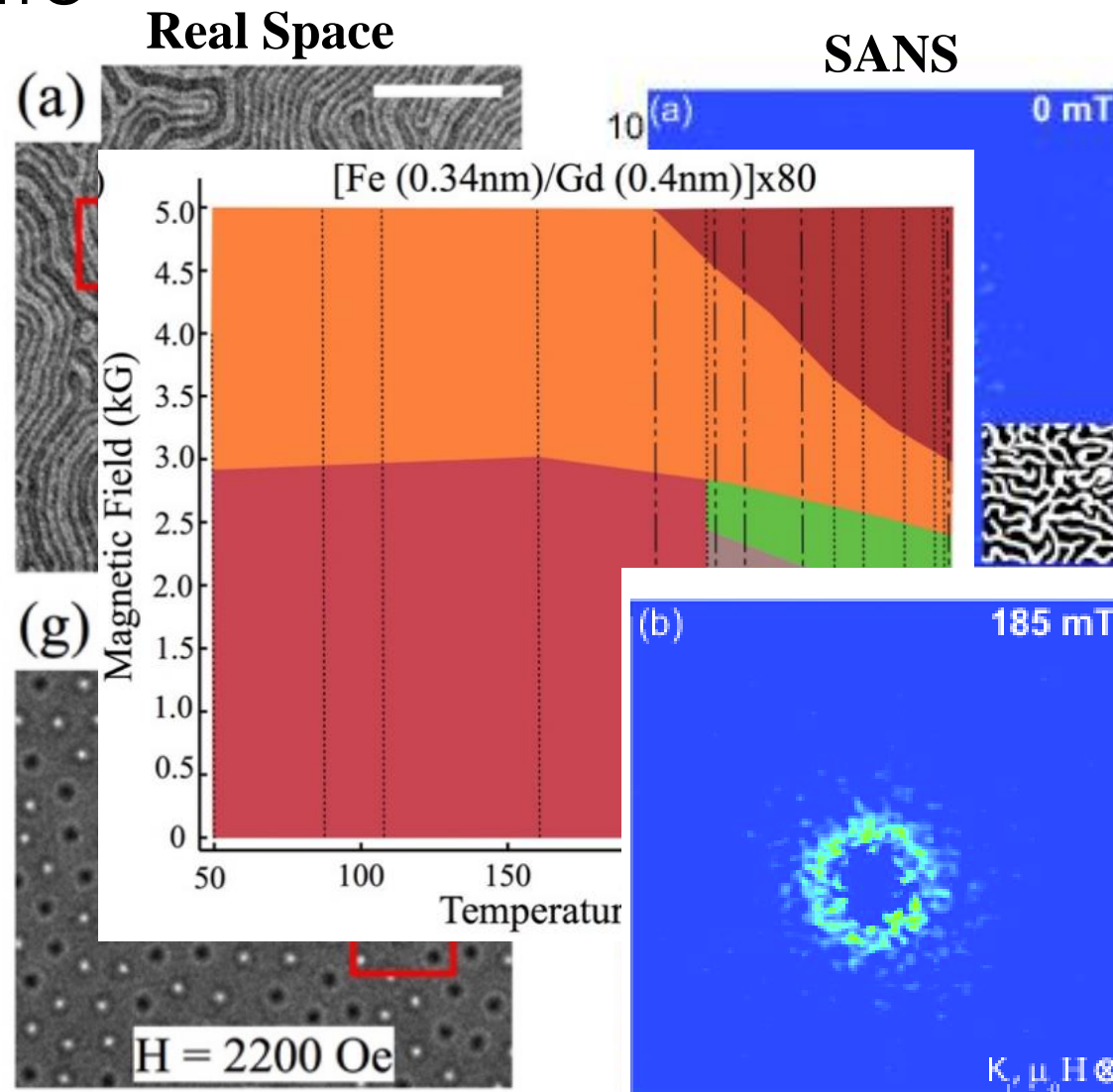
Limited/no DMI

**No in-plane structure to cement
a long-range orientation**

Forming the Skyrmion State



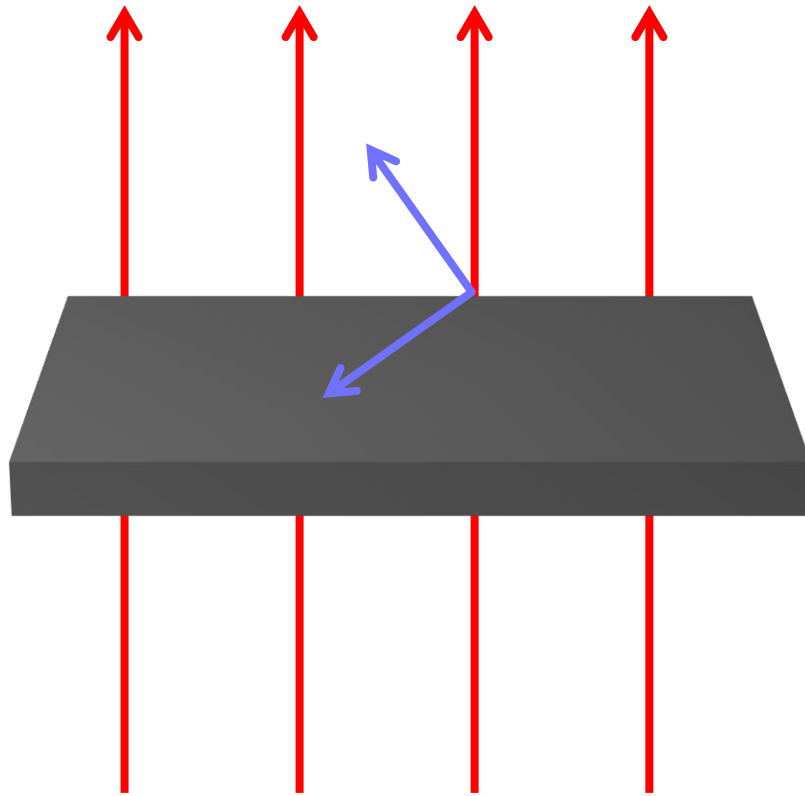
Montoya *et al.*, Phys. Rev. B **95**, 024415 (2017)



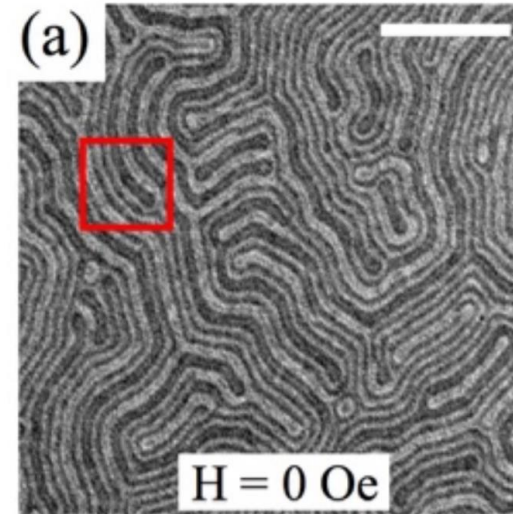
From saturation, worm domain remanent state

Break up into chiral bubbles, no chirality control, no long range order

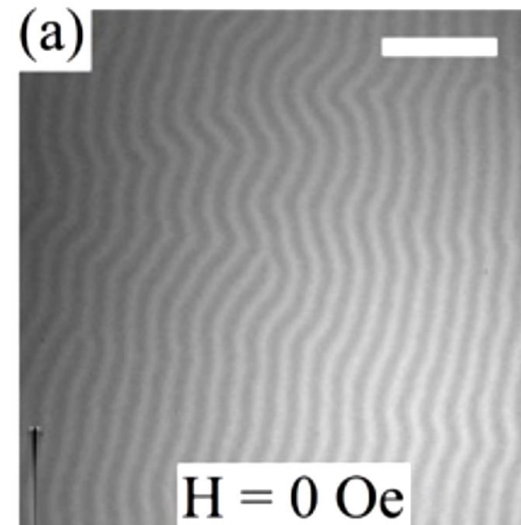
Generating an Artificial Striped Phase



Applied Field



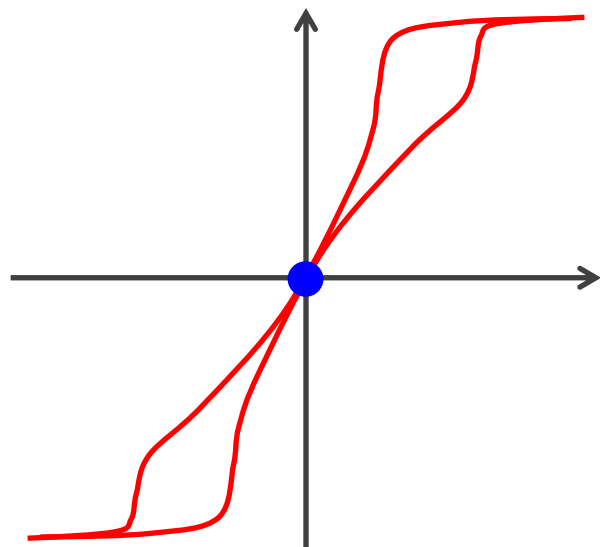
Labyrinth (or worm) domains



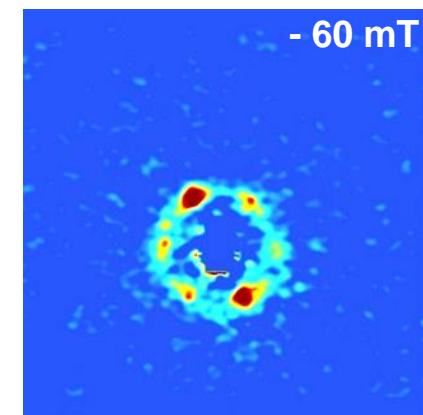
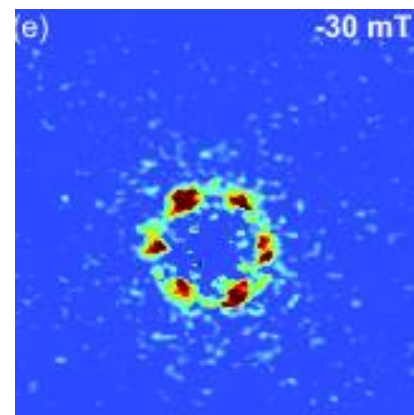
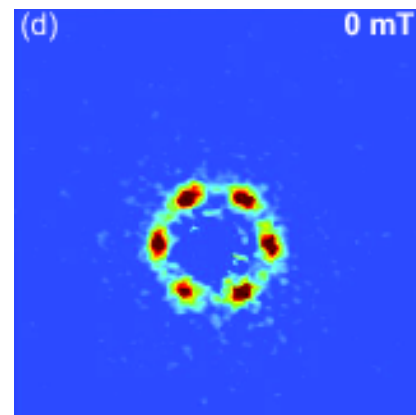
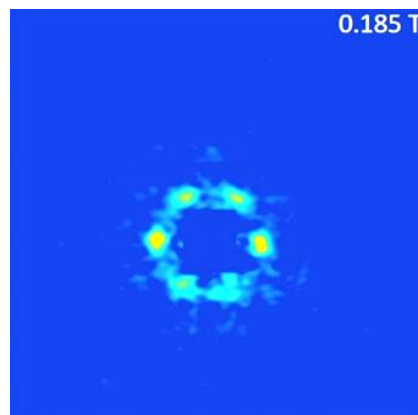
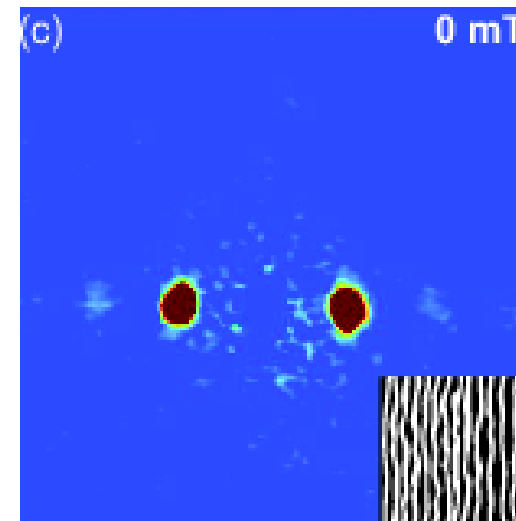
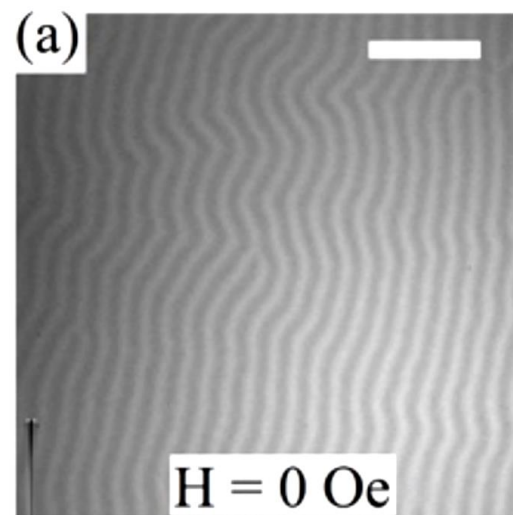
Tilting the sample imparts an in-plane field which breaks the symmetry

Artificial Stripe Domain

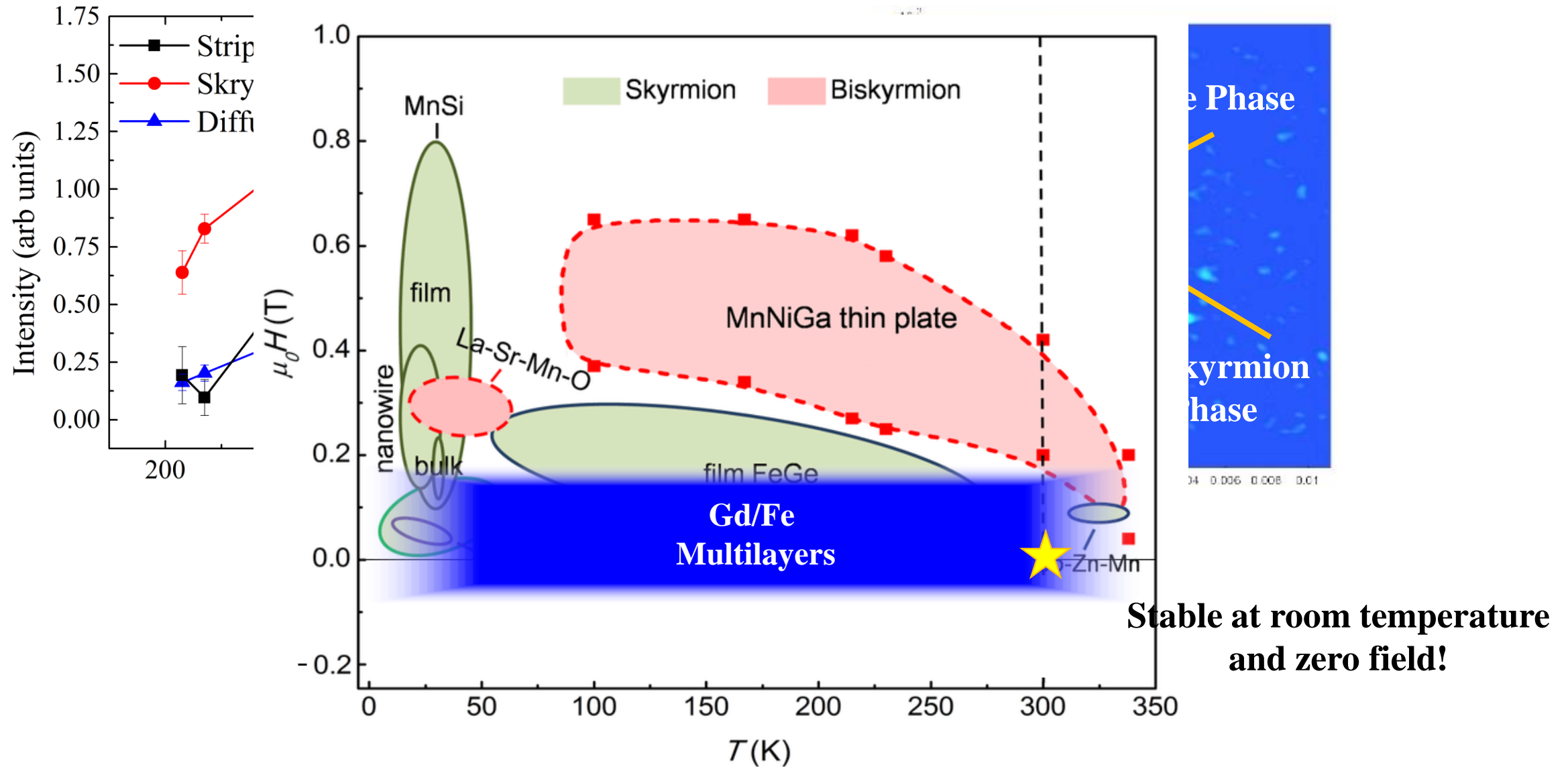
Generating an Artificial Striped Phase



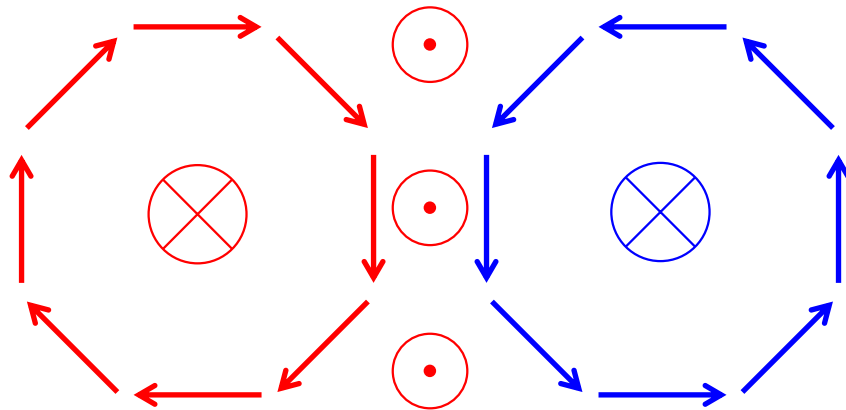
Desautels et al., *Under Review*



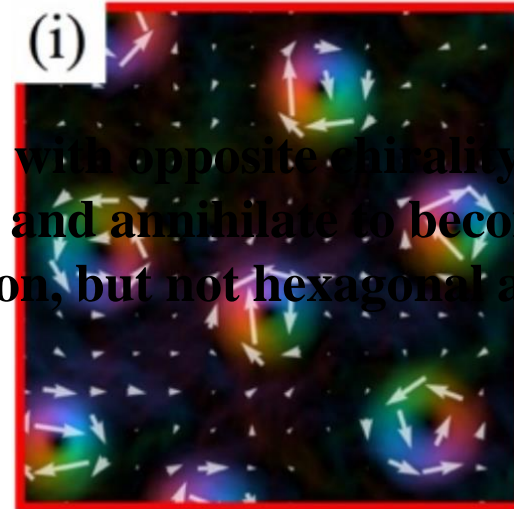
Skyrmion lattice Stability Envelope



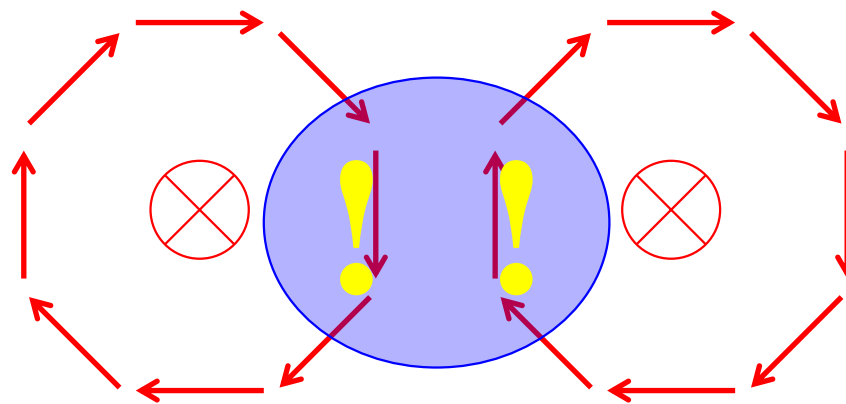
Implications of Chirality Control on the stability of Skyrmion Lattices



TEM indicates Bloch-type structure with no circularity control



Bubbles with opposite chirality will coalesce and annihilate to become a biskyrmion, but not hexagonal arrays

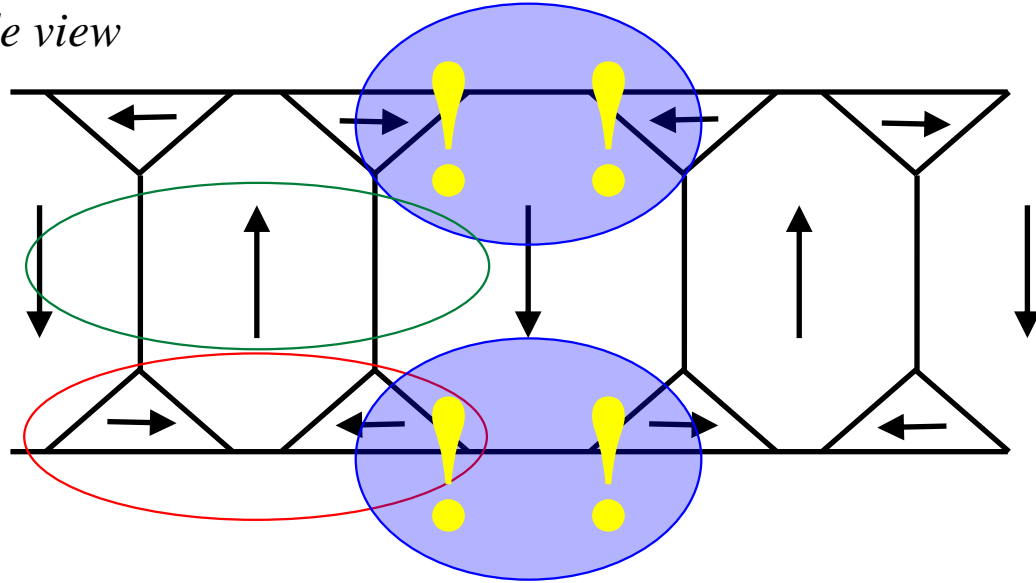


Strong repulsive interactions between bubbles with identical chirality

→ Hexagonally Ordered Arrays

Implications of Chirality Control on the stability of Skyrmion Lattices

Side view



**Appears as Néel Skyrmion, not Bloch
(as observed with TEM)**

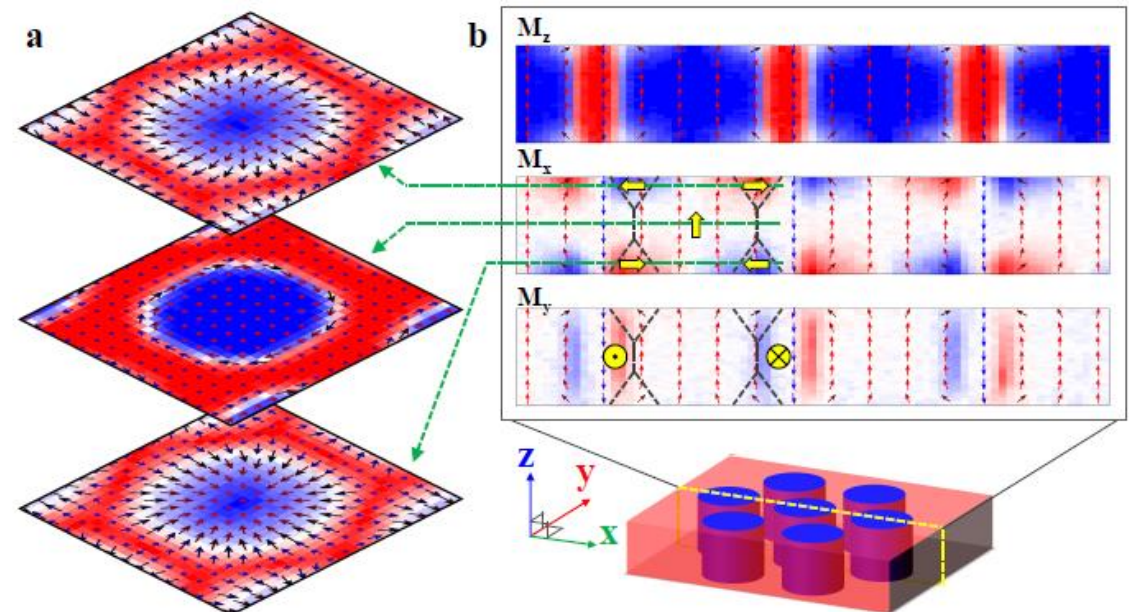
**Maybe Neel on the top and bottom,
Bloch in the middle**

**Without DMI, the Bloch region has no
net chirality (as observed in TEM)**

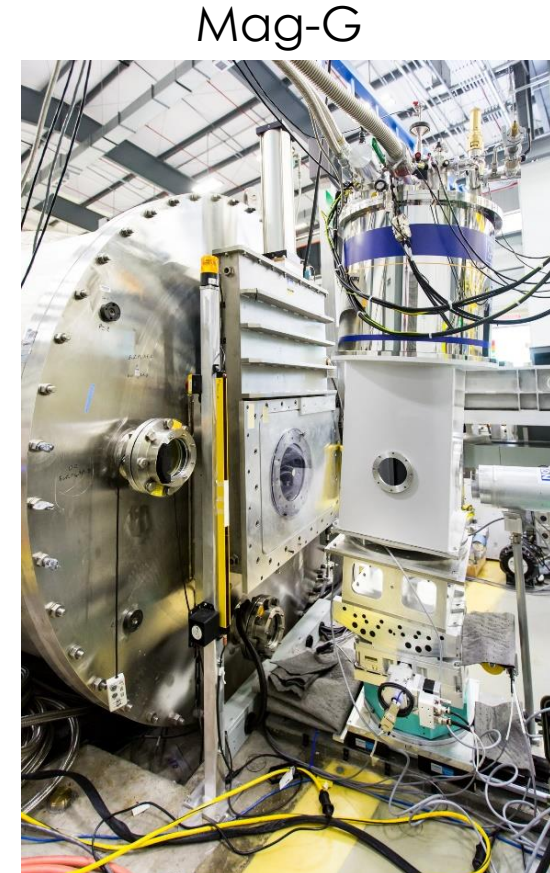
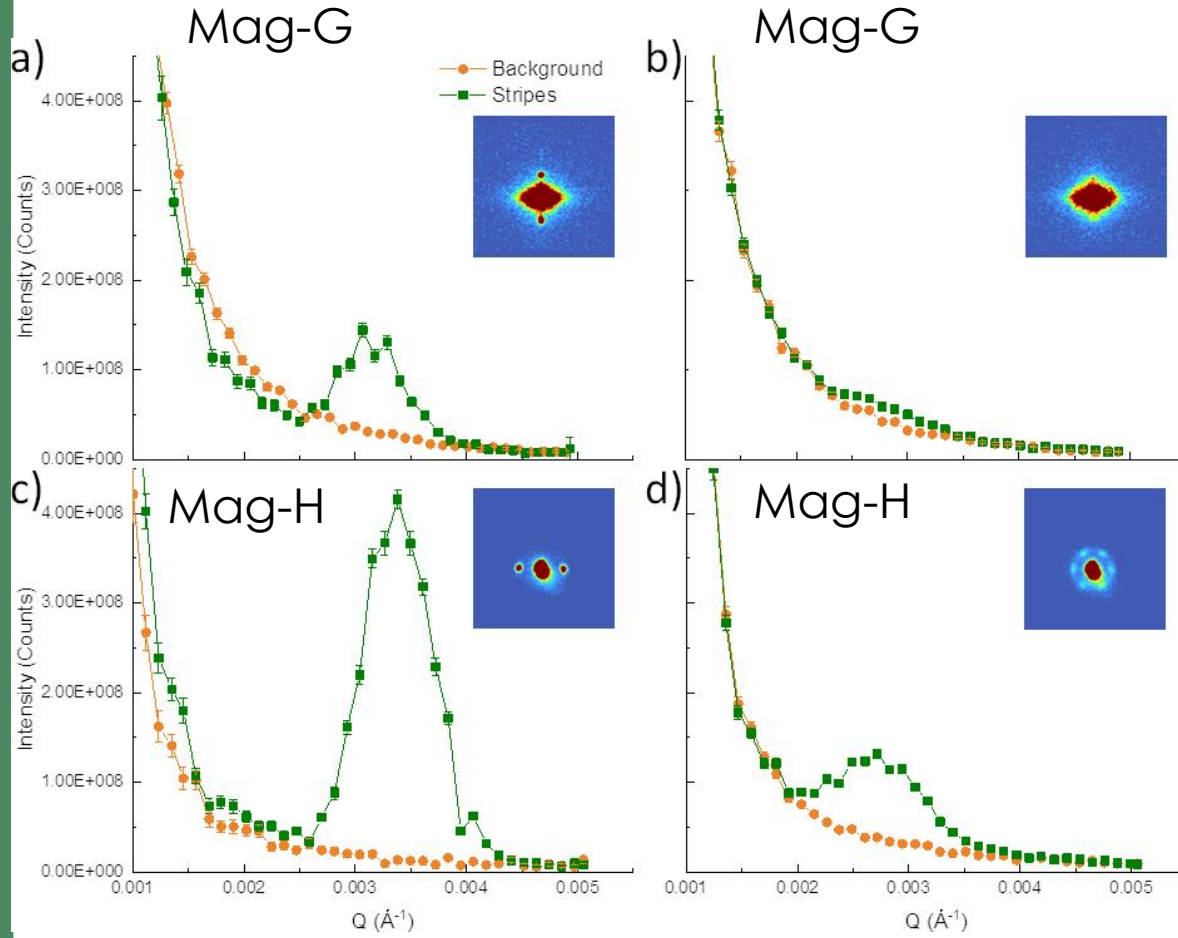
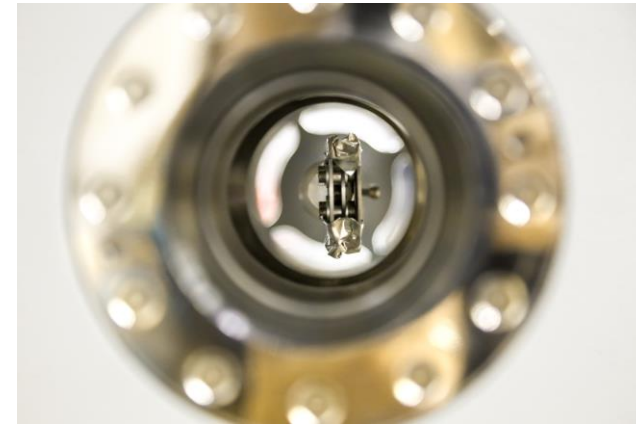
**Assumed these are flux-closure
domains with no defined chirality**

Strong Repulsive Interaction

**Repulsive interactions due to surface features,
which have their chirality defined by the dipole
fields**



Thin Films studies at GP-SANS



Use of Small-Angle Neutron Scattering to Characterize Novel Steels for Reactor Applications

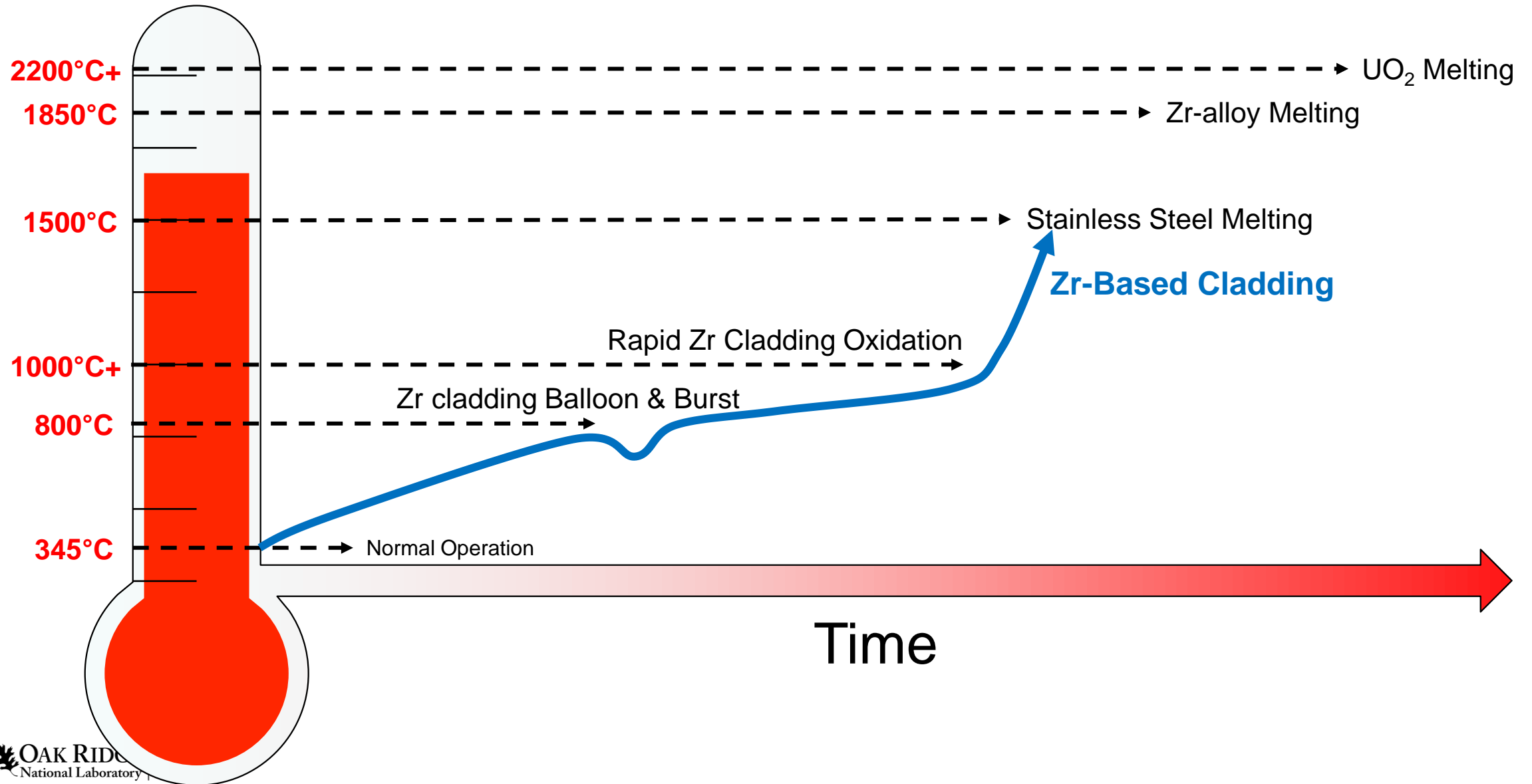
Kevin G. Field¹, Kenneth C. Littrell^{1*}, and Samuel A. Briggs²

¹Oak Ridge National Laboratory

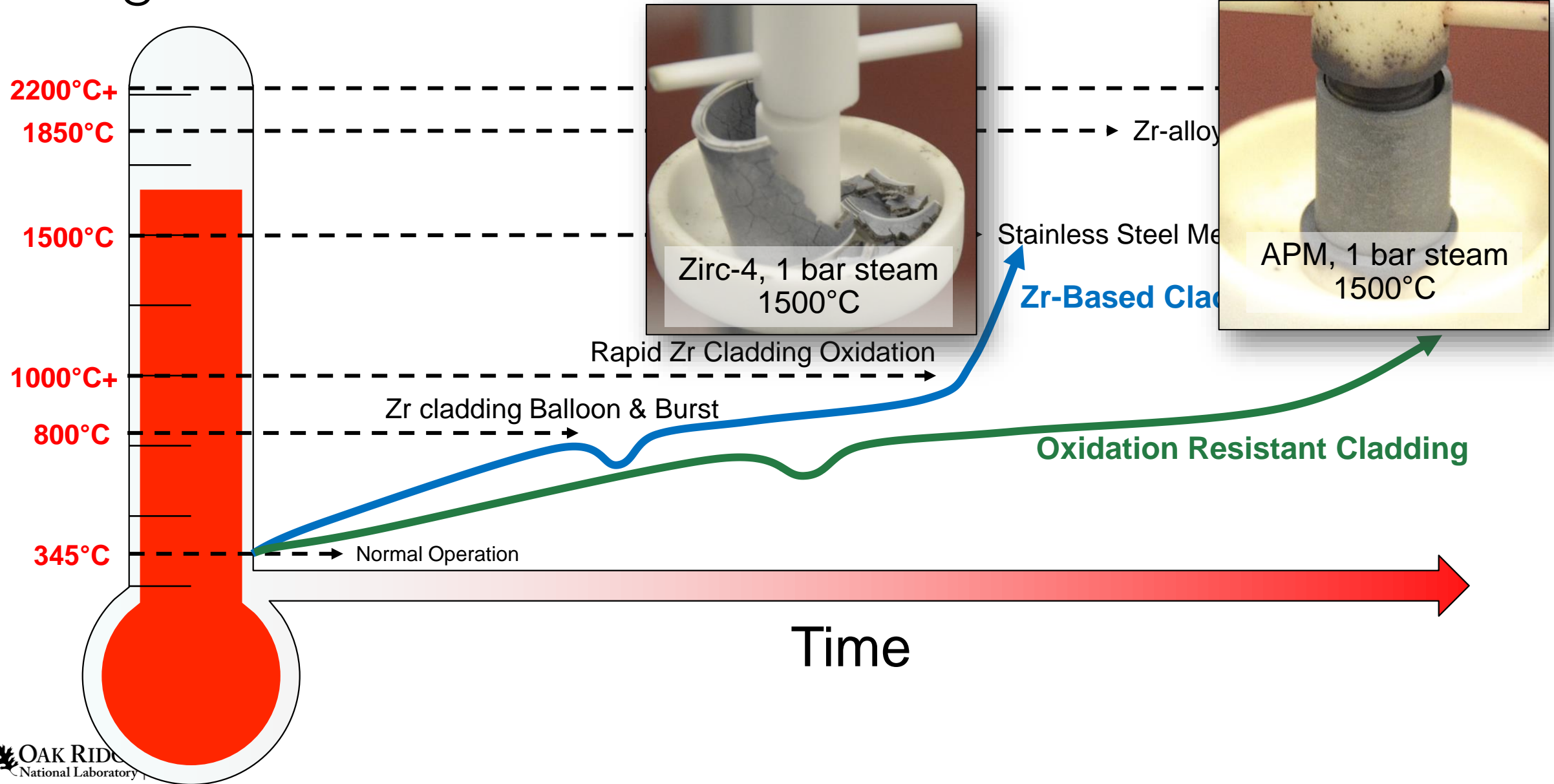
²Sandia National Laboratories

ORNL is managed by UT-Battelle, LLC for the US Department of Energy

Oxidation of cladding is key towards core degradation during a coolant-limited accident scenario



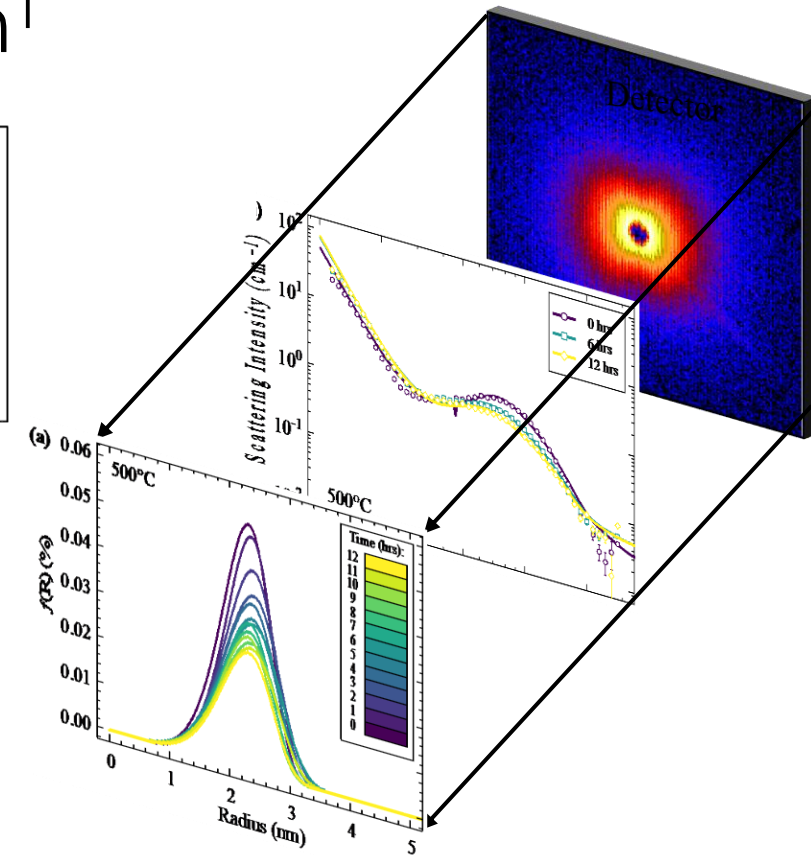
Oxidation of cladding is key towards core degradation during a coolant-limited accident scenario



SANS Scattered Intensity: Local Monodispersed Approximation¹

$$\frac{d\sigma}{d\Omega}(q) = \Delta\rho^2 \int_0^\infty \phi(q, R)^2 S[q, R_{HS}(R)] N(R) dR + Aq^{-B} + C$$

- Contrast: $\Delta\rho^2 = (\rho_{particle} - \rho_{matrix})^2$
- Form factor (for spheres):
 $\phi(q, R) = 3V_0[\sin(qR) - qR\cos(qR)]/(qR)^3$
- Structure factor: $S[q, R_{HS}(R)] = [1 + 24\eta_{HS}G(R_{HS}q)/(R_{HS}q)]^{-1}$
- Size distribution (Weibull density function): $N(R) = (R/\bar{R})^{b-1} \exp[-(R/\bar{R})^b]$
- Low-q power-law: Aq^{-B}
- Background: C



Magnetic Shielded-SANS measurements : Contrast from Neutrons

1. Nuclear contrast:

$$\Delta\rho_{nucl}^2 = (\rho_{nucl,particle} - \rho_{nucl,matrix})^2$$

2. Magnetic contrast:

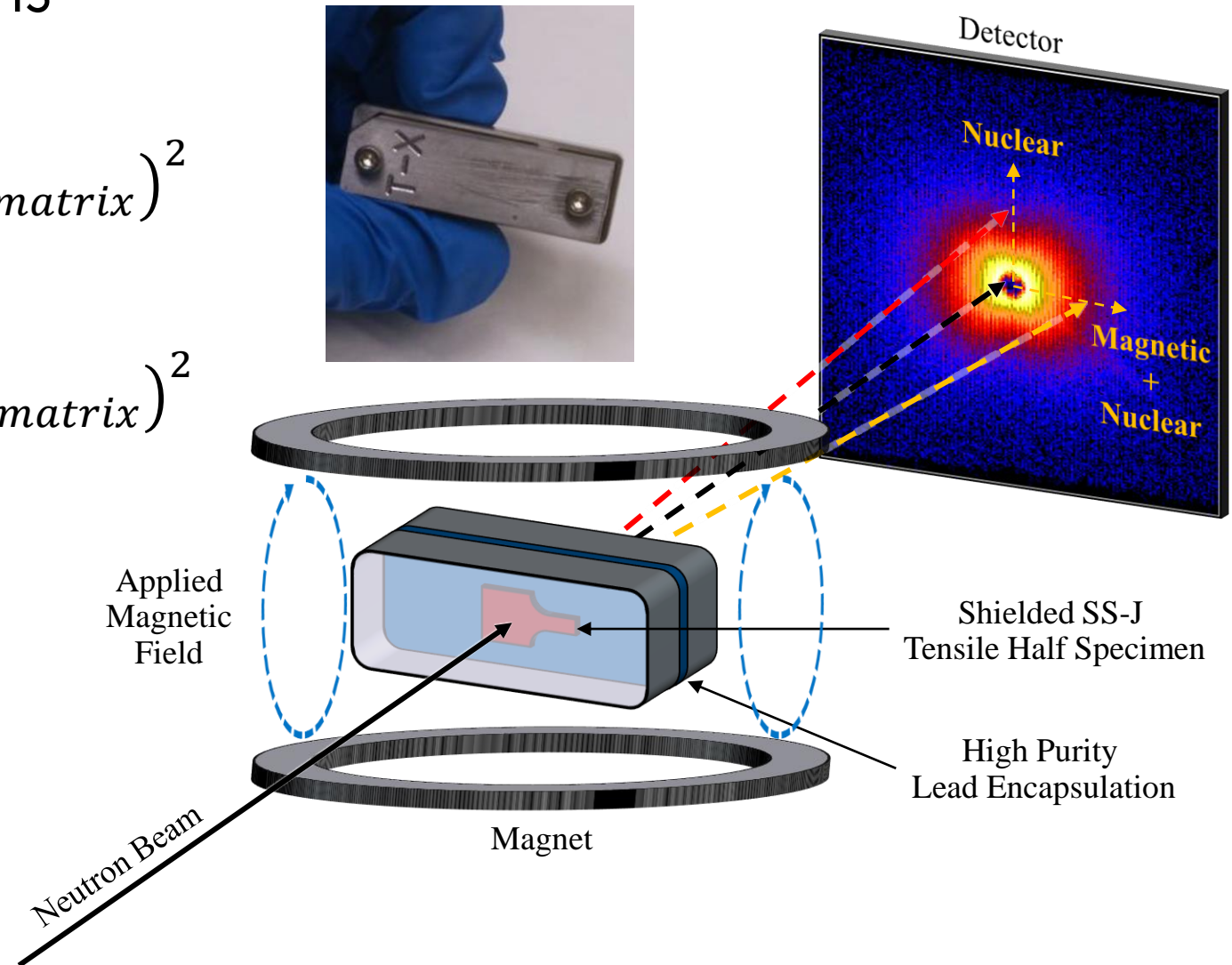
$$\Delta\rho_{mag}^2 = (\rho_{mag,particle} - \rho_{mag,matrix})^2$$

$$\frac{d\sigma}{d\Omega}(q) = \Delta\rho^2 \int_0^\infty \phi(q,R)^2 \dots \square$$



$$[\Delta\rho_{nucl}^2 + \Delta\rho_{mag}^2 \sin^2 \alpha]$$

**Can exploit magnetization
to extract composition**



Radiation tolerance of FeCrAl alloys is analogous to FeCr alloys under similar irradiation conditions

Change in Yield Strength

Burgers Vector

Number Density

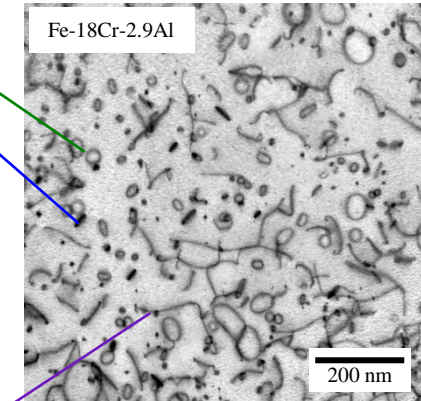
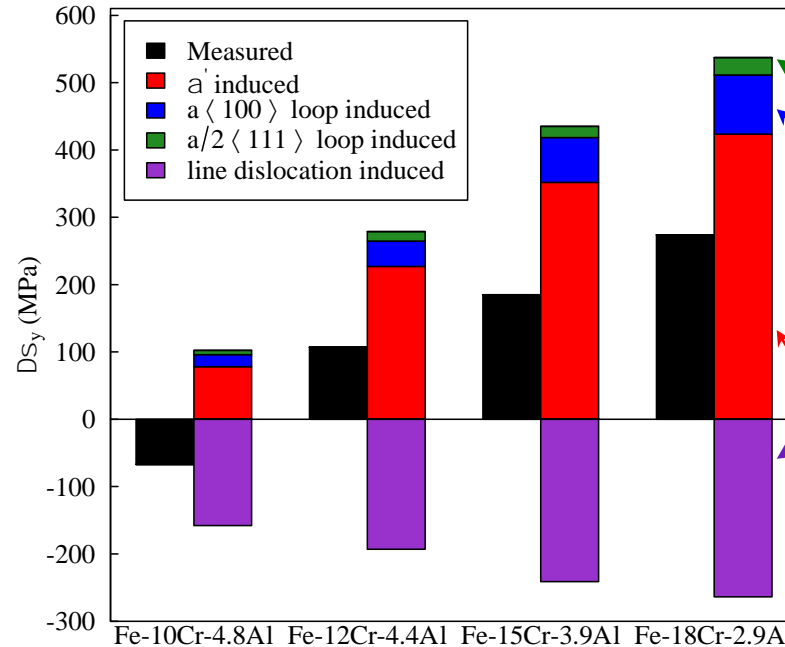
Size

Taylor Factor

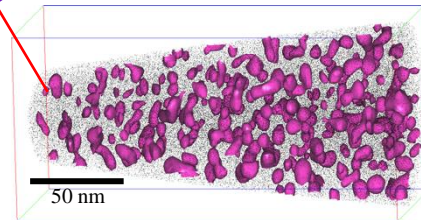
Shear Modulus

$$\Delta\sigma_y = M\alpha\mu b\sqrt{\rho \cdot d}$$

Super. rule	Barrier strength of visible defects (a)			
	Cr-rich α'	$\langle 100 \rangle$	$\frac{1}{2}\langle 111 \rangle$	Line
Linear	0.04	0.31	0.05	0.68
SRS	0.06	0.33	0.17	0.56



STEM image showing dislocation loops and line dislocations in 1.8 dpa, 382°C irradiated Fe-18Cr-2.9Al alloy



APT reconstruction showing α' in 1.8 dpa, 382°C irradiated Fe-18Cr-2.9Al alloy

- Dispersed barrier hardening (DBH) has linked radiation-hardening in FeCrAl alloys to formation of Cr-rich α' and dislocation loops after neutron irradiation to 1.8 dpa at 382°C

Need exists to understand the role of composition and temperature on the formation and progression of Cr-rich α' in FeCrAl alloys

A large amount of FeCrAl samples have been irradiated and/or tested over the past 5 years...



...how do we characterize α' from these efficiently?

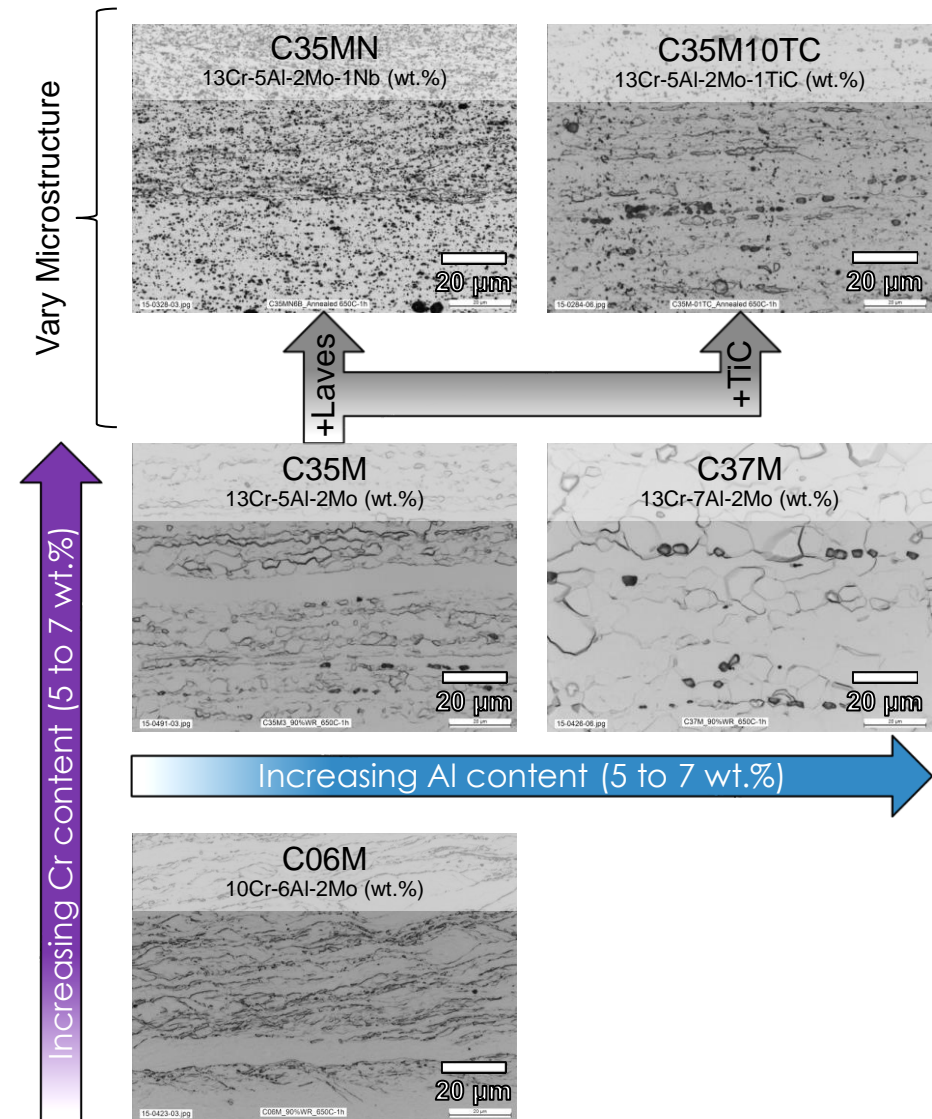
Magnetic Shielded-SANS measurements: Role of temperature and composition on α'

- Selected FeCrAl alloys irradiated in HFIR to determine temperature, composition, and microstructure trends

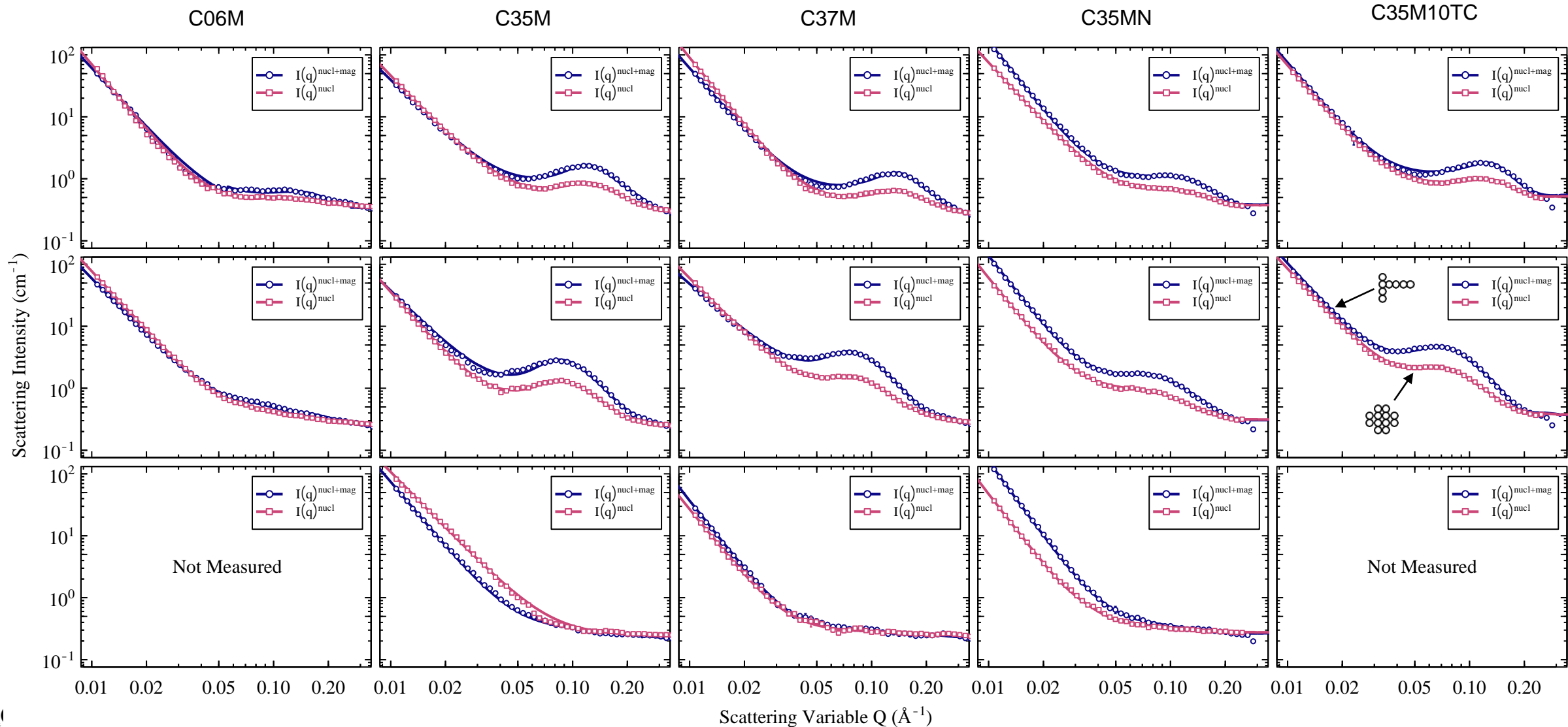
Capsule ID	Number Samples	Neutron Flux (n/cm ² s) E > 0.1 MeV	Neutron Fluence (n/cm ²) E > 0.1 MeV	Dose Rate (dpa/s)	Dose (dpa)	Irradiation Temperature (°C)
FCAT-01	45	1.10×10^{15}	2.17×10^{21}	9.6×10^{-7}	1.9	194.5 ± 37.9
FCAT-02	45	1.04×10^{15}	2.05×10^{21}	9.1×10^{-7}	1.8	362.7 ± 21.2
FCAT-03	45	1.10×10^{15}	2.17×10^{21}	9.6×10^{-7}	1.8	559.4 ± 28.1

Increasing Temp.

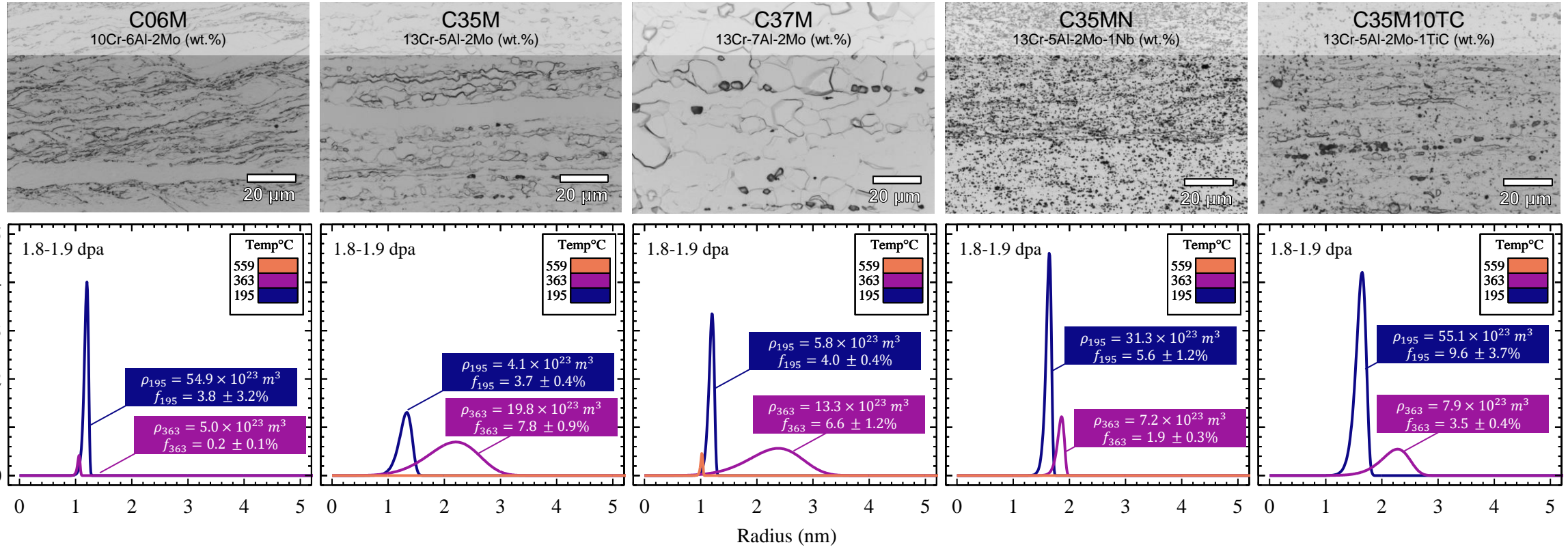
- Measurements performed at CG-2 general purpose SANS beamline at HFIR
- Data collected on broken tensile heads in magnetic shielded SANS configuration



Magnetic Shielded-SANS measurements: Role of temperature and composition on a'



Magnetic Shielded-SANS measurements: Role of temperature and composition on α'



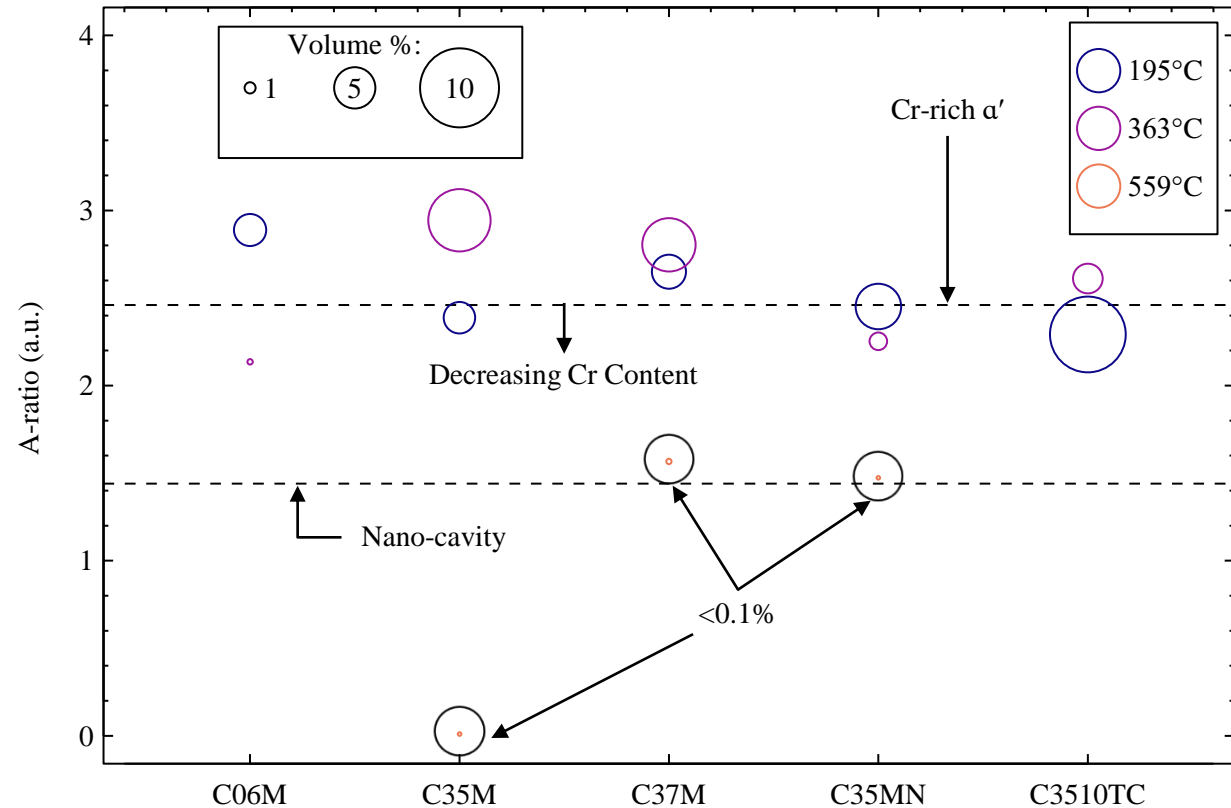
- Increasing irradiation temperature increases mean radius and distribution width
- Cr stronger than Al in control in α' precipitation
- Microstructure (precipitates/grain size) can play a role in α' precipitation

Magnetic Shielded-SANS measurements: Role of temperature and composition on α'

$$\frac{d\sigma}{d\Omega}(q) = \Delta\rho^2 \int_0^\infty \phi(q, R)^2 \dots \square$$

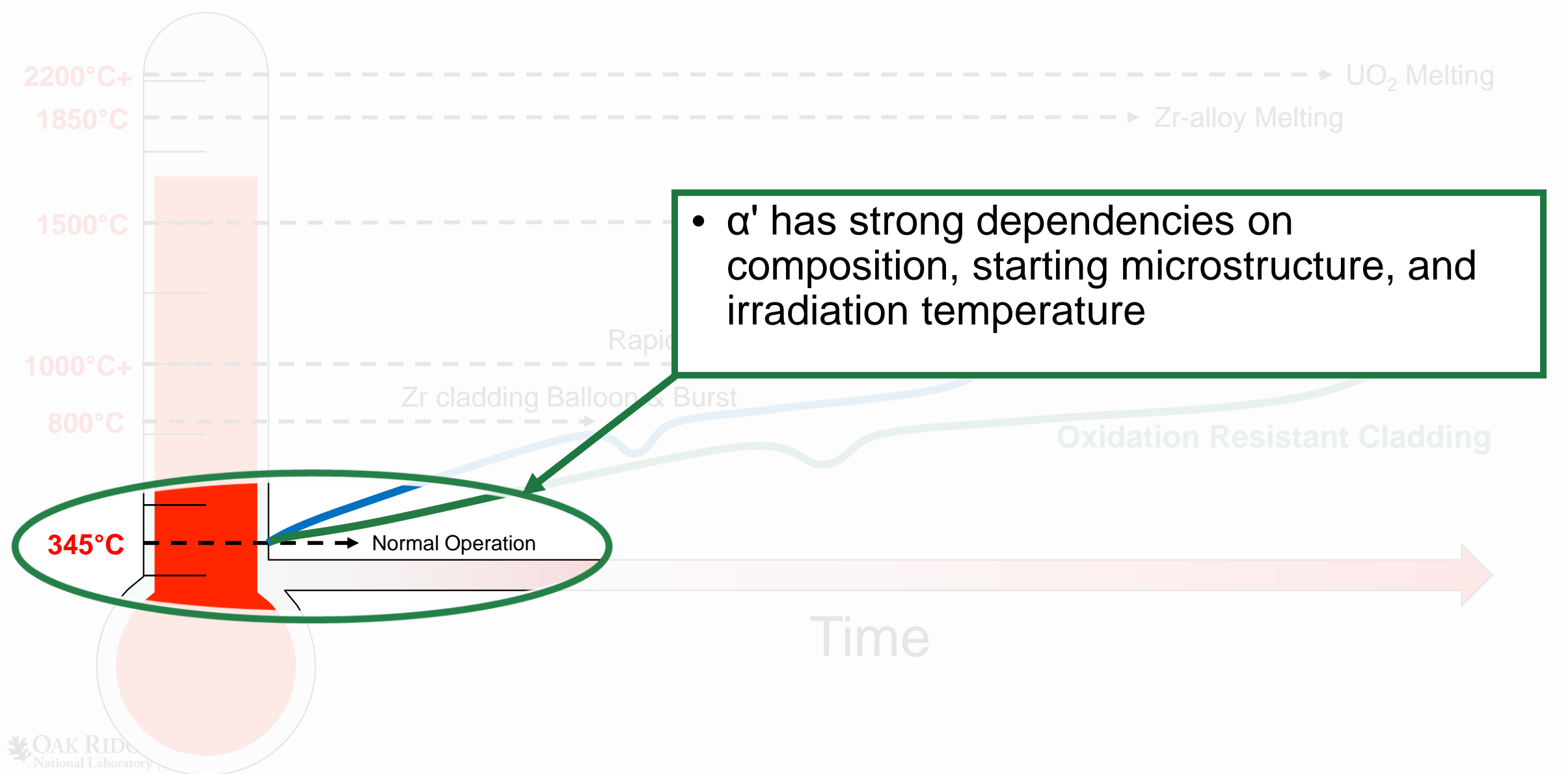
$$[\Delta\rho_{nucl}^2 + \Delta\rho_{mag}^2 \sin^2 \alpha]$$

$$A - ratio = \frac{\Delta\rho_{mag+nucl}^2}{\Delta\rho_{nucl}^2}$$



- Magnetic shielded SANS reveals that irradiations below 500°C form primarily α'
 - Typically lower Cr content in 195°C irradiations
- Above 500°C, scattering could be from nano-cavity formation

Practical Application of Ex-situ SANS results: α' concern for normal operation, but can be tuned

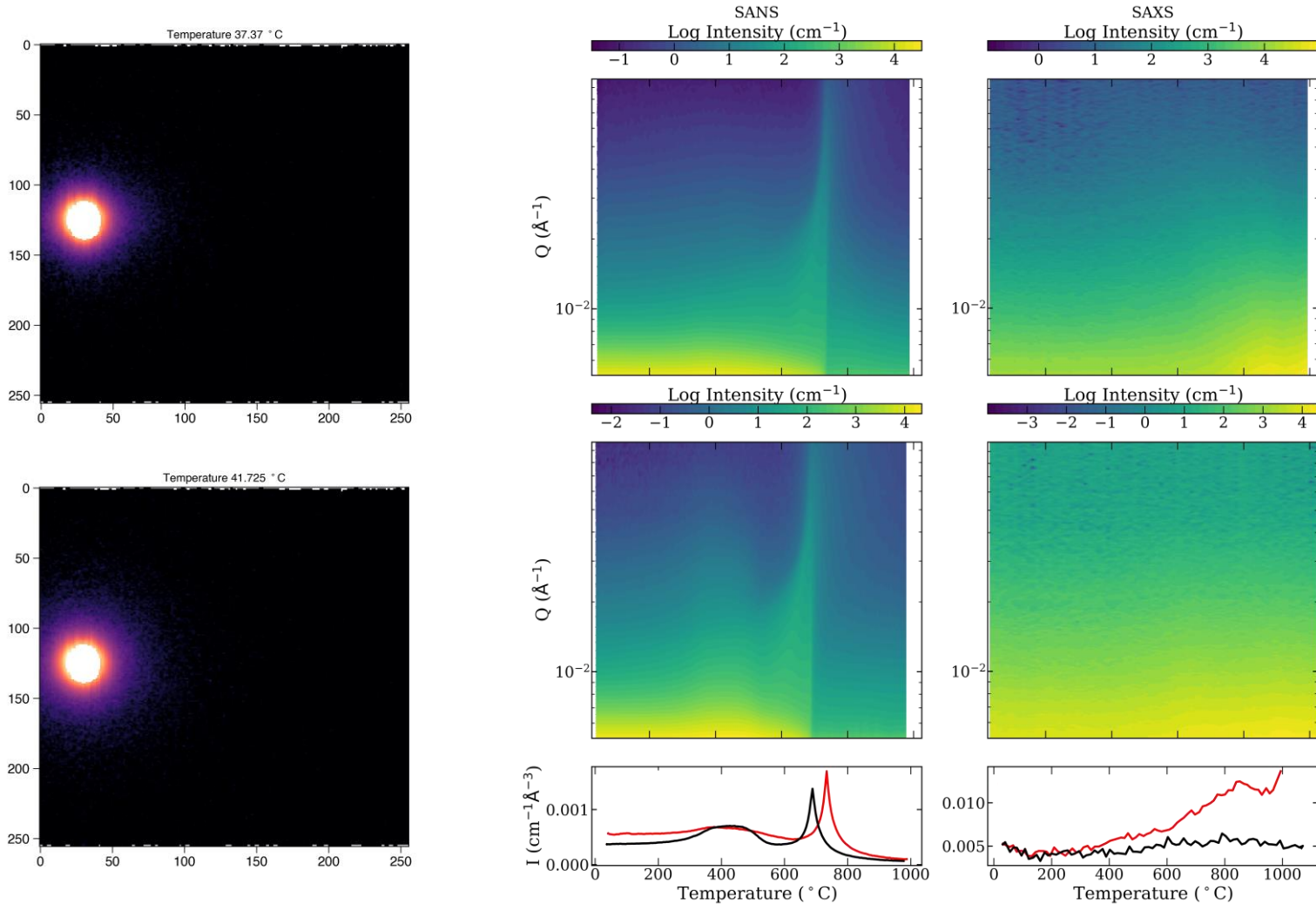


New Directions with SANS

- Time-resolved SANS
- GI-SANS



Time-resolved SANS (TR-SANS)

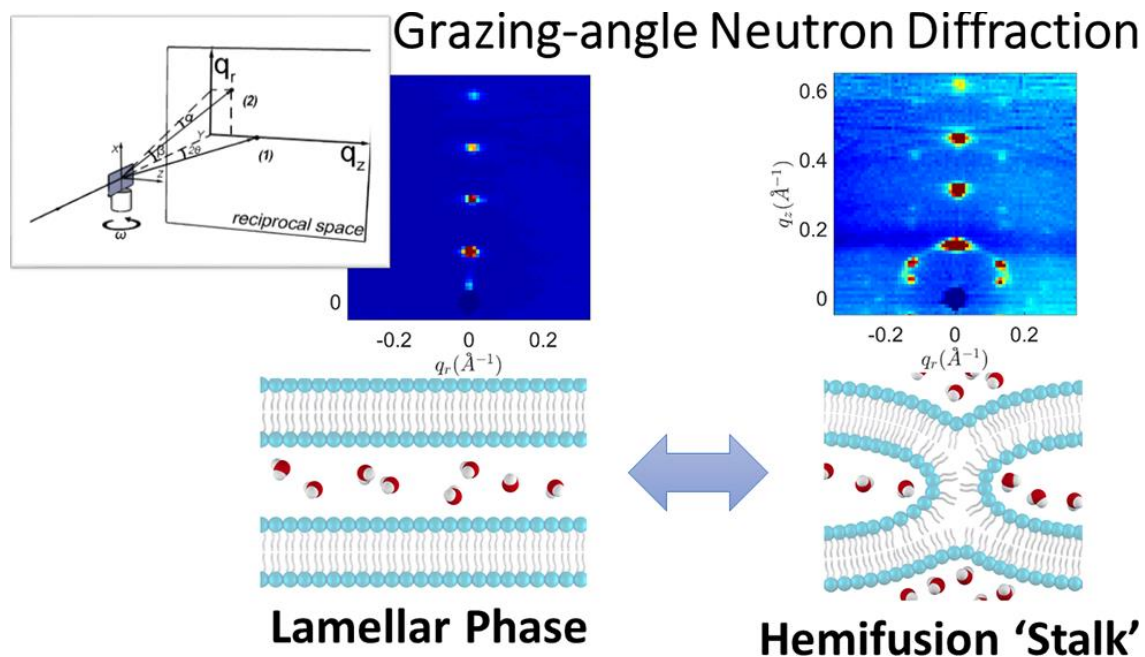


- Additively manufactured steels
- Data collected during ramp, 5 hour anneal, and cooling(not shown)
- SANS and SAX data taken under same heat treatment
- SANS sees metastable magnetic domain changes, but SAXS is only sensitive to the microstructure evolution

C. Fancher *et al.* In preparation

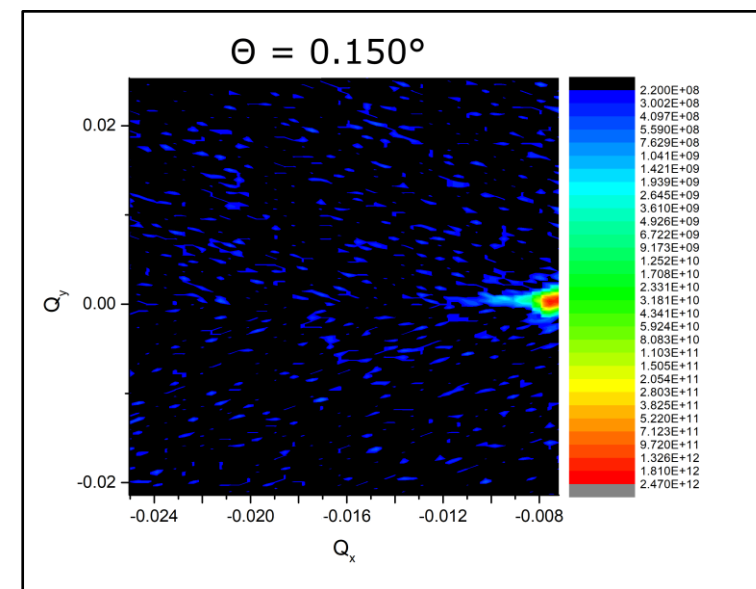
GI-SANS

- Being developed at ORNL at EQ-SANS but GP-SANS, BIO-SANS can do this technique.
- Measuring the specular and off-specular versus sample angle encodes both in-plane and out-of-plane structure of the systems.



S. Qian and D. K. Rai J. Phys. Chem. Lett. 2018, 9, 5778-5784

Fe/Gd multilayers measured with a large (195 mT) out-of-plane field in the skyrmion phase



WLNC Liyanage *et. al* in preparation

Experts at ORNL on GI-SANS:

- Shuo Qian
- Changwoo Do
- Valeria Lauter

Thank you for your attention.

- SANS is powerful tool for probing mesoscale structures in a multitude of systems
- ORNL SANS have a wide variety of sample environments to enable your science

Questions?

Instrument Teams:

GP-SANS



Lisa
DeBeer-Schmitt



Ken
Littrell



Lilin
He



Cody
Pratt

Bio-SANS



Venky
Pingali



Wellington
Leite



Volker
Urban



Luke
Heroux

USANS



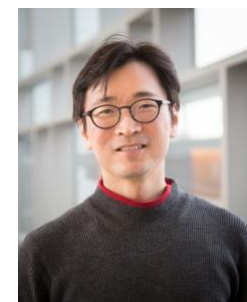
Wei-ren Chen



Yingrui Shang



Carrie Gao



Changwoo Do



William Heller



Gergely Nagy

EQ-SANS

